

GLOBAL STABILITY AND LOCAL BIFURCATIONS IN A TWO-FLUID MODEL FOR TOKAMAK PLASMA

D. ZHELYAZOV ^{*}, D. HAN-KWAN [†], AND J.D.M. RADEMACHER [‡]

Abstract. We study a two-fluid description for high and low temperature components of the electron velocity distribution in an idealized tokamak plasma evolving on a cylindrical domain, and taking into account nonlinear drift effects only. We refine previous results on the laminar steady state stability and include viscosity. Taking the temperature difference as the primary parameter we show that linear instabilities and bifurcations occur within a finite interval and for small enough viscosity only, while the steady state is globally stable for parameters sufficiently far outside the interval. We find that primary instabilities always stem from the lowest spatial harmonics for aspect ratios of poloidal vs. radial extent below some value larger than 2. Moreover, we show that any codimension-one bifurcation of the laminar state is supercritical, yielding spatio-temporal oscillations in the form of travelling waves, hence locally stable for such bifurcations destabilizing the laminar state. In the degenerate case, where the instability region in the temperature difference is a point, these solutions form an arc connecting the bifurcation points. We also provide numerical simulations to illustrate and corroborate the analysis, and find additional bifurcations of the travelling waves.

1. Introduction. Existence of coherent states and their stability are fundamental questions in tokamak plasma theory and application, see, e.g., [3, 7, 10, 16–18]. We study stability and bifurcations in a simple model for high and low temperature phases near the plasma edge, which appears in [20] and is a viscous variant of the model derived in [10]. It captures nonlinear effects due to electric drift in the magnetic field, the ‘ $E \times B$ ’ drift, and the electron temperature gradient only. Our results highlight the role of these selected effects and give detailed information, which seem currently not possible for the much more accurate Vlasov-Maxwell or Vlasov-Poisson models considered in, e.g. [3, 18].

A fundamentally important effect in tokamaks is the confinement for strong $E \times B$ -drift, the so-called H-mode [4]. In accordance with this effect, the laminar conducting state of the model we study turns out to be globally (in phase space) stable for sufficiently large temperature difference, analogous to the result in [10]. In agreement with numerically observed spatio-temporal oscillations in [20] we show that for moderate temperature difference, the linear instabilities generically create dynamically stable periodic travelling waves, which attract all perturbations of the laminar state at least near onset. Hence, in this model, the loss of confinement is associated initially with transport through travelling waves. Concerning the more complicated dynamics mentioned in [20], we conjecture these result from secondary bifurcations, which arise when decreasing viscosity from large values that suppress all instabilities: Unfolding the emergence of an unstable parameter region initially gives an arc of stable solutions, which connects the bifurcations at the interval endpoints. Numerical computation show that increasing viscosity can generate secondary instabilities on the continuation of this arc, and also the co-existence of the stable laminar state with (unstable) oscillations.

We believe the analysis in this paper is also interesting from a mathematical per-

^{*}Centrum Wiskunde & Informatica, Science Park 123, 1098 XG Amsterdam. FOM Institute DIFFER - Dutch institute for fundamental energy research, Association EURATOM-FOM, P.O. Box 1207, 3430 BE Nieuwegein, the Netherlands

[†]CNRS and Centre de Mathématiques Laurent Schwartz, Ecole polytechnique 91128 Palaiseau Cedex, daniel.han-kwan@polytechnique.edu.

[‡]Universität Bremen, Fachbereich 3 – Mathematik, Postfach 33 04 40, 28359 Bremen, Germany, rademach@math.uni-bremen.de

spective, providing a non-trivial case of a nonlocal (after solving the Poisson equation) spatially two-dimensional parabolic evolution equation transitioning from global stability to pattern forming local bifurcations, which we analyze by PDE estimates, and spectral analysis combined with center manifold reduction, respectively. We provide a much more detailed analysis compared to the hyperbolic model variant with unit aspect ratio studied in [10], and apply different techniques.

Mathematical model. The model equations for the miscible phases ρ^\pm of ‘hot’ and ‘cold’ plasma with constant temperatures $T^+ > T^- > 0$, and the electric potential V read

$$\begin{cases} \partial_t \rho^+ = T^+ \partial_{x_2} \rho^+ - E^\perp \cdot \nabla \rho^+ + \nu_+ \nabla^2 \rho^+, \\ \partial_t \rho^- = T^- \partial_{x_2} \rho^- - E^\perp \cdot \nabla \rho^- + \nu_- \nabla^2 \rho^-, \\ E = -\nabla V, \\ -\nabla^2 V = \rho^+ + \rho^- - 1, \end{cases} \quad (1.1)$$

where $\nu_+, \nu_- > 0$, $E^\perp = (E_2, -E_1)^T$. The equations are posed on the cylindrical domain

$$x = (x_1, x_2) \in [0, L_1] \times \mathbb{R}/L_2\mathbb{Z},$$

subject to the Dirichlet boundary conditions

$$\begin{aligned} V(0, x_2, t) = V(L_1, x_2, t) = 0, \\ \rho^\pm(0, x_2, t) = \rho_{ss}^\pm(0), \rho^\pm(L_1, x_2, t) = \rho_{ss}^\pm(L_1), \end{aligned} \quad (1.2)$$

that respect the ‘laminar’ steady state

$$\rho_{ss} = (\rho_{ss}^+, \rho_{ss}^-), \rho_{ss}^+(x_1) := 1 - \frac{x_1}{L_1}, \rho_{ss}^-(x_1) := \frac{x_1}{L_1} \quad (1.3)$$

of (1.1) for which the electric potential and field vanish.

System (1.1) derives from a drift kinetic model, describing the interaction between drifts for plasma of different temperatures in a slab with one periodic direction. See [10, (1.5)] and (up to a reflection) equivalently [20, (1)]. Here the configuration space is 2D in position and 1D in velocity and we refer the reader to [19], [20] for a discussion of the physics. Concerning equations for the potential we refer to the introduction of [11].

There are at least two possibilities to obtain the two-fluid model from the kinetic equations. The first one, following [10], approximates the distribution function of electrons by two Dirac-distributions in 1D velocity space, that is,

$$f(x, v, t) \approx \rho^+(x, t) \frac{\delta(|v| - \sqrt{2T^+})}{2\pi\sqrt{2T^+}} + \rho^-(x, t) \frac{\delta(|v| - \sqrt{2T^-})}{2\pi\sqrt{2T^-}}, \quad (1.4)$$

which yields (1.1) for $\nu^\pm = 0$ as a hyperbolic system of PDE, whose nonlinear terms stem from the electric field driving ρ^\pm via the ‘ $E \times B$ drift’ of all charged particles. Accounting for viscosity gives (1.1) with $\nu_\pm > 0$ as a parabolic PDE system.

The second possibility to derive (1.1), following [20], is to consider a certain moment closure of the fluid hierarchy. The resulting equations have the form of a two-fluid system with equal viscosity coefficients, which agrees with (1.1) for $\nu_+ = \nu_-$: the fluid equations in (1.1) and [20, (6)] are equivalent in that case. Therefore, we will focus on the case of small $\Delta\nu := \nu_- - \nu_+$ and write $\nu := \nu_+$, $\nu_- := \nu + \Delta\nu$.

Relations to other models. Before a more detailed discussion of the results of this paper, we briefly discuss some relations to other models. Taking a mathematical perspective, we may interpret the deviations of hot and cold electron densities from the laminar state (see also (2.1) below) as vorticities ω with the velocity vector field $(\nabla(\nabla^2)^{-1}(\omega_1 + \omega_2))^\perp$. Then system (1.1) can be interpreted as 2D Navier-Stokes with two vorticities, vorticity sources and an advection term generated by ΔT , cf. [2].

For the comparison with related physical models, it is useful to change variables

$$\rho^+ = \frac{1 + \nabla^2\psi + \theta}{2}, \quad \rho^- = \frac{1 + \nabla^2\psi - \theta}{2}, \quad V = -\psi \quad (1.5)$$

and pass to the co-moving frame $x_2 \rightarrow x_2 - \frac{T^+ + T^-}{2}t$. For $\Delta\nu = 0$ system (1.1) then becomes

$$\begin{aligned} \partial_t \nabla^2\psi + [\psi, \nabla^2\psi] - \frac{\Delta T}{2} \partial_x \theta - \nu \nabla^4\psi &= 0, \\ \partial_t \theta + [\psi, \theta] - \frac{\Delta T}{2} \partial_x \nabla^2\psi - \nu \nabla^2\theta &= 0, \end{aligned} \quad (1.6)$$

with $x_1 = z$ and $x_2 = x$ and the Poisson bracket $[f, g] = \partial_x f \partial_z g - \partial_z f \partial_x g$. The Dirichlet boundary conditions (1.2) become

$$\psi = \partial_{zz}\psi = 0, \quad \text{for } x_1 = 0, L_1, \quad \text{and } \theta(0, x_2, t) = -\theta(L_1, x_2, t) = \frac{1}{2}. \quad (1.7)$$

This form readily shows similarities but also highlights differences to several related models. In particular, we see that the Hasegawa-Wakatani equations [13, (5)-(6)], a well-known model for resistive drift wave turbulence near the plasma edge derived from mode coupling, differs in several terms. Also the related models of shear flow and shear induced stability that we are aware of differ from (1.6), e.g., [9], and more recently [25]. Only a single term in (1.6) differs from Saltzman's model [21, (16'), (17')] of Rayleigh-Bénard convection in the Boussinesq approximation, which is a classical widely studied model that exhibits pattern formation bifurcations: the term $-\frac{\Delta T}{2} \partial_x \nabla^2\psi$ in (1.6) is replaced by $-\frac{\Delta T_0}{H} \frac{\partial \psi}{\partial x}$ in [21, (17')]. However, boundary conditions and basic steady state are also different in the literature.

Despite these differences, a common feature in particular with the Saltzman model is the emergence of periodic travelling waves through bifurcations. Notably, the $SO(2)$ translation symmetry of (1.1) in x_2 implies that bifurcations of Hopf-type are steady state bifurcations in a suitable co-moving frame; see §5. Moreover, for steady states (1.1) with equal viscosities and in a suitable co-moving frame possesses a reflection symmetry and hence an $O(2)$ -symmetry. Such an $O(2)$ -symmetry can also be present e.g. in the Saltzman model, cf. [15], and implies that the bifurcating travelling waves have a stronger steady state character with velocity predicted by the linear problem. However, the reflection symmetry is broken for differing viscosities and we therefore rely on the center manifold reduction for Andronov-Hopf bifurcations.

Laminar steady state. The relevance of the laminar steady state ρ_{ss} was already noted in [10] for $\nu^\pm = 0$ and $L_1 = L_2 = L$ without the Dirichlet boundary conditions (1.2). In that case it is linearly unstable in a bounded interval $(\Delta T_1, \Delta T_2) = (0, \frac{4L}{5\pi^2})$ of the parameter $\Delta T = T^+ - T^-$ and linearly stable for $\Delta T \notin [\Delta T_1, \Delta T_2]$. Not surprisingly, this structure persists for moderate viscosity with modified thresholds $\Delta T_1 = \mathcal{O}((\nu^\pm)^2)$, $\Delta T_2 = 4L/(5\pi^2) + \mathcal{O}((\nu^\pm)^2)$, see Fig. 1.1. In addition to studying

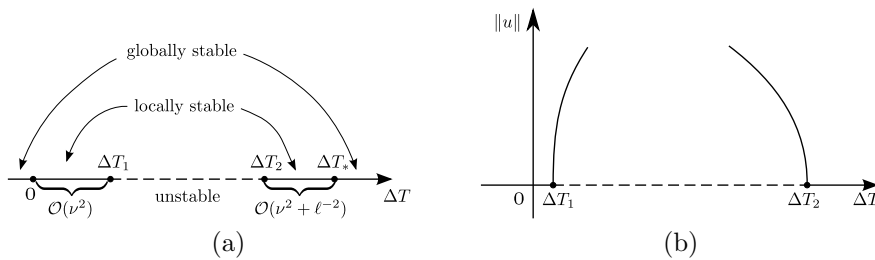


FIG. 1.1. (a) Schematic illustration of the main case of a primary 1-instability region in the stability analysis of the steady state ρ_{ss} when including equal viscosities. The estimate of the global stability threshold ΔT_* is larger than the linear stability threshold, even at $\nu = 0$. However, in the limit $\nu \rightarrow 0$ the lower thresholds coincide, and if in addition $\ell \rightarrow \infty$, then also the upper linear thresholds tend to the global ones. (b) Sketch of local bifurcation diagram of the steady state $u = 0$ with supercritical branches of stable limit cycles. Solid line represents stable solutions and dashed lines unstable ones.

linear stability and instability, it was shown in [10] that the laminar steady state is actually globally stable for $\Delta T < 0$ and $\Delta T > \Delta T_* = 4L/\pi^2$ (in the sense of \mathbf{L}^2 -space convergence). Here $\Delta T_* > \Delta T_2$ is an *estimate* for a global stability threshold, which may not be sharp.

One of the original motivations for the present paper was to explain the necessity of a difference between the local (linear) and a global (fully nonlinear) stability threshold through *subcritical* bifurcations at ΔT_2 . In such a case, the global stability threshold must be larger than the linear one due to the presence of non-zero amplitude solutions that do not converge to the laminar state. We prove, however, that the bifurcations are always *supercritical*. Of course, a difference in thresholds can still be due to other nonzero amplitude solutions that the local bifurcation analysis cannot reveal and indeed we present numerical evidence for such solutions in §8.2.

Nontrivial aspect ratios $L_2 \neq L_1$ provide additional insight into the threshold relation, which is also motivated from the modelling point of view as a thin strip near the plasma edge, where $0 < L_1 \ll L_2$. We show that for $\nu^\pm = 0$ the upper linear stability threshold ΔT_2 of the lowest spatial harmonics and the estimated global stability thresholds become

$$\Delta T_2 = \frac{4L_1L_2^2}{\pi^2(L_2^2 + 4L_1^2)} = \frac{4\ell^2L_1}{(4 + \ell^2)\pi^2}, \quad \Delta T_* = \frac{4L_1}{\pi^2},$$

so that ΔT_* is in fact independent of L_2 . Now we notice that the estimate of the global stability threshold ΔT_* is related to the upper linear stability threshold via

$$\lim_{\ell \rightarrow \infty} \Delta T_2 = \Delta T_*,$$

so that the discrepancy is smaller on thinner domains. Note that as a (estimated) global stability threshold, ΔT_* is always an upper bound for a linear instability in ΔT .

Coming back to the model origins, the sign of ΔT can be related to the region within the tokamak that is modelled by (1.1): ‘good curvature’ (negative ΔT) and ‘bad curvature’ (positive ΔT) regions, which is consistent with the different stability properties for positive and negative ΔT as noted in [10] – the model captures the electron temperature gradient instability. Our rigorous results are in agreement with

the instability (L-mode) being present for moderate temperature gradients on the bad curvature side only, and being suppressed for large enough gradients [4]. But the modelling and physical relations, in particular to L-H transition (see [22]) remain to be understood. “Clearly, the model selection criteria, apart from the sound physics behind them, should be based on their capability to reproduce key experimental facts such as spontaneous L-H transitions, characteristic intermediate regimes (such as dithering), or hysteresis” [16].

Main results. In this paper, we pursue a mathematical analysis that may serve as a basis to investigate further the model assessment and relations to physical phenomena. Our main results with $\nu^\pm > 0$ may be summarized as follows, see Fig. 1.1 for illustration.

Global stability (Theorem 7.3) The steady state ρ_{ss} is globally exponentially L^2 -stable for $\Delta T < 0$ and $\Delta T > \Delta T_* = \frac{4L_1}{\pi^2} \max\left(\frac{\nu_-}{\nu_-}, \frac{\nu_-}{\nu_+}\right)$.

Local bifurcations (Theorems 4.1, 4.3) For $0 \leq \Delta\nu \ll 1$ and parameter sets including $L_2/L_1 < 2\sqrt{2} \approx 2.8$ the following holds.

At the stability thresholds ΔT_j , $j = 1, 2$, the critical modes are spatially the lowest harmonics, and supercritical periodic travelling wave bifurcations occur (with $O(2)$ -symmetry for $\Delta\nu = 0$) yield waves with velocity $\frac{1}{2}(T^+ + T^-) + \mathcal{O}(\Delta\nu)$ at onset.

Near the degenerate case $\Delta T_1 = \Delta T_2$ the two bifurcating branches of travelling waves are connected (in ΔT), and form an arc of stable periodic solutions. We numerically corroborate that, further away from this degeneracy, secondary symmetry-breaking bifurcations occur along the arc (Figure 8.4).

In case $L_2 \gg L_1$, the primary instabilities can also be higher spatial harmonics, even simultaneously, but for codimension-1 cases the supercriticality remains valid (Remark 5, Corollary 3.5, Theorem 4.4). We thus suspect rich dynamics already at onset for ‘thin’ domains, but a detailed analysis is beyond the scope of this paper. It is also possible that, as ΔT increases, a sequence of destabilization and restabilization occur through different harmonics (Lemma 3.7).

Finally, on the infinite strip $[0, L_1] \times \mathbb{R}$, the laminar state undergoes supercritical Turing-type instabilities (Lemma 5.1).

This paper is organized as follows. In §2 we reformulate the problem for a subsequent bifurcation analysis. Section 3 concerns the spectrum of the linearized operator in the steady state ρ_{ss} . In §4 we discuss the center manifold reduction, reduced vector fields and prove the main bifurcation results. In §5 we explain the relation to travelling wave bifurcations, and consider pattern formation as well as Turing instabilities in case of an infinite strip. In §6 we discuss nonlinear instability for $\nu^\pm \geq 0$ in the linearly unstable region. §7 contains the global stability result. Finally, section 8 contains numerical computations, illustrating the results.

Acknowledgement. This work, supported by the European Communities under the contract of Association between EURATOM/FOM, was carried out within the framework of the European Fusion Programme with financial support from NWO. The views and opinions expressed herein do not necessarily reflect those of the European Commission. D.H.-K. is grateful to the CWI, where this work was initiated, for its hospitality. J.R. has been supported in part by NWO cluster NDNS+ and thanks his previous employer, CWI, where a large part of the work has been done. D.Z. gratefully acknowledges hospitality at the University of Bremen. The authors thank Hugo de Blank for his comments and suggestions on a draft version, and the reviewers as well as the editor for their helpful comments.

2. Reformulation and setting. For the bifurcation study it is convenient to formulate (1.1) through the deviation $u = (u_1, u_2)$ from ρ_{ss} ,

$$\rho^+ = u_1 + \rho_{ss}^+, \rho^- = u_2 + \rho_{ss}^-.$$

In terms of u , and in the comoving variable $x_2 \rightarrow x_2 + T^-t$, system (1.1) reads

$$\begin{cases} \partial_t u_1 = \Delta T \partial_{x_2} u_1 + E_2/L_1 - E^\perp \cdot \nabla u_1 + \nu \nabla^2 u_1, \\ \partial_t u_2 = -E_2/L_1 - E^\perp \cdot \nabla u_2 + (\nu + \Delta \nu) \nabla^2 u_2, \\ E = -\nabla V, \\ -\nabla^2 V = u_1 + u_2, \\ x \in [0, L_1] \times \mathbb{R}/L_2\mathbb{Z}, t \geq 0, \end{cases} \quad (2.1)$$

subject to (periodic b.c. in x_2 and) homogeneous Dirichlet boundary conditions

$$\begin{aligned} u_1(0, x_2, t) = u_2(0, x_2, t) = V(0, x_2, t) = 0, \\ u_1(L_1, x_2, t) = u_2(L_1, x_2, t) = V(L_1, x_2, t) = 0. \end{aligned} \quad (2.2)$$

REMARK 1. *The aforementioned reflection symmetry for $\Delta \nu = 0$ occurs in the reference frame with speed $-\frac{1}{2}\Delta T$ in (2.1), which yields the advection terms $\sigma_j(\frac{1}{2}\Delta T \partial_{x_2} u_j + E_2/L_1)$, $\sigma_1 = 1, \sigma_2 = -1$ in the equation for u_1, u_2 , respectively. Here the system possesses the reflection symmetry $(u_1, u_2, x_1, x_2) \mapsto (u_2, u_1, -x_1, -x_2)$ so that the set of solutions invariant under the symmetry forms an invariant subspace. Together with the translation symmetry in x_2 the system thus has $O(2)$ -symmetry and the solutions emerging from codimension-one bifurcations lie in this subspace, thus having a priori determined velocity $-\frac{T^+ + T^-}{2}$ in (1.1). Notably, these solutions are non-stationary for typical T^+, T^- , and the symmetry is broken for $\Delta \nu \neq 0$.*

REMARK 2. *A peculiarity of the Poisson bracket nonlinearity in (1.1) and equivalently (2.1) is that, viewed on complexified phase space, each eigenspace of the laplacian is flow invariant and the dynamics is purely linear. Indeed, take an eigenfunction e with eigenvalue $-\lambda$ of the laplacian and set $u_j = \alpha_j e$ with $\alpha_j \in \mathbb{C}$ so that $E = (\alpha_1 + \alpha_2)/\lambda \nabla e$. Hence, $E^\perp \cdot \nabla u_j = 0$ so that (2.1) is in fact linear. Noting that E_2 is a multiple of an eigenfunction implies the claim. (For the explicit formulas of e see g_k below.) In particular, x_2 -independent u_1, u_2, V form an invariant subspace, which follows also immediately from the translation symmetry in the x_2 -direction. The reduced evolution on this space given by the uncoupled heat equations $\partial_t u_1 = \nu \partial_{x_1}^2 u_1$, $\partial_t u_2 = (\nu + \Delta \nu) \partial_{x_1}^2 u_2$ together with the then trivial $-\partial_{x_1}^2 V = u_1 + u_2$.*

However, this is the only case of such flow invariant eigenspaces for the real equations since all other eigenvalues and eigenspaces of the linear part of (2.1) are complex (see Lemma 3.1 below).

REMARK 3. *Concerning boundary conditions, the spectral analysis of the linear part of (2.1) in §3 below also covers zero-flux boundary conditions on one side of the domain: doubling the domain extends the sine basis functions in x_1 -direction to the homogeneous Dirichlet case of (2.1). However, the image of an eigenfunction under the nonlinearity violates such boundary conditions.*

Next we choose a simple functional analytic setting for a formulation of (2.1) as a parabolic problem by solving the Poisson equation. This is convenient for the center manifold reduction, but also gives a simple well-posedness setting.

Let $\Omega := [0, L_1] \times [0, L_2]$ and denote the Sobolev spaces $\mathbf{H}^j = H^j([0, L_1] \times \mathbb{R}/L_2\mathbb{Z})$ as well as

$$\begin{aligned} X &:= H_0^1([0, L_1] \times \mathbb{R}/L_2\mathbb{Z}), \\ Y &:= \{f \in \mathbf{H}^2 : f(0, x_2) = f(L_1, x_2) = 0\}, \\ Z &:= \{f \in \mathbf{H}^3 : f(0, x_2) = f(L_1, x_2) = 0\}, \end{aligned} \tag{2.3}$$

which incorporate the boundary conditions. We shall use standard notation: for $f_1, f_2 \in L^2([0, L_1] \times \mathbb{R}/L_2\mathbb{Z})$ we denote the scalar product by $\langle f_1, f_2 \rangle = \int_{\Omega} f_1(x) \overline{f_2(x)} dx$ and for $\mathbf{f}_j = (f_{j,1}, f_{j,2}) \in (L^2([0, L_1] \times \mathbb{R}/L_2\mathbb{Z}))^2$ $j = 1, 2$ by $\langle \mathbf{f}_1, \mathbf{f}_2 \rangle_2 = \langle f_{1,1}, f_{2,1} \rangle + \langle f_{1,2}, f_{2,2} \rangle$.

Thanks to these boundary conditions we can solve the Poisson equation in (2.1); see also §3 for explicit solutions. We thus obtain E via the bounded operators $A_j : Z \rightarrow \mathbf{H}^3$ defined by

$$\begin{aligned} A_j f &:= \partial_{x_j} (\nabla^2)^{-1} f, \quad j = 1, 2, \\ A f &= (A_1 f, A_2 f)^T, \\ A^\perp f &= (A_2 f, -A_1 f)^T. \end{aligned} \tag{2.4}$$

Notably, A_2 in fact maps into Z , because $E_2 = \partial_{x_2} V$ vanishes for $x_1 = 0, L_1$ due to the Dirichlet boundary conditions.

In order to apply standard results on parabolic equations, let us write (2.1) equivalently in the standard form

$$\frac{du}{dt} = \mathbf{L}u + R(u), \tag{2.5}$$

so that solutions of this and (1.1) are in 1-to-1 correspondence. Here

$$\begin{aligned} \mathbf{L}u &= \begin{pmatrix} \Delta T \partial_{x_2} u_1 + \frac{1}{L_1} A_2 (u_1 + u_2) + \nu \nabla^2 u_1 \\ -\frac{1}{L_1} A_2 (u_1 + u_2) + (\nu + \Delta \nu) \nabla^2 u_2 \end{pmatrix}, \\ R(u) &= \begin{pmatrix} -A^\perp (u_1 + u_2) \cdot \nabla u_1 \\ -A^\perp (u_1 + u_2) \cdot \nabla u_2 \end{pmatrix}. \end{aligned}$$

Note that $\mathbf{L} \in \mathcal{L}(Z \times Z, X \times X)$ is the linearization of (1.1) in ρ_{ss} . We have that $R : Z \times Z \rightarrow Y \times Y$ since $\nabla u_j \in \mathbf{H}^2 \times \mathbf{H}^2$ and $-A^\perp (u_1 + u_2) \cdot \nabla u_j$ vanish at $x_1 = 0, L_1$, and \mathbf{H}^2 is a Banach algebra; R is in fact analytic in u . See also §4. Moreover, the imbeddings $Z^2 \hookrightarrow Y^2 \hookrightarrow X^2$ are dense and the uniformly elliptic operator $-\mathbf{L} : Z \times Z \subset X \times X \rightarrow X \times X$ is a sectorial operator, generating an analytic semigroup, and so (2.1) admits mild and classical solutions $u(t)$ for any initial condition $u(0) \in Y \times Y$. The sectoriality is a consequence of the fact that the laplacian is sectorial in Y with domain L^2 of the cylinder [14], and this is robust under addition of the lower order terms in \mathbf{L} . It thus also possesses a square root, which then provides an isomorphism from L^2 to X . Hence, \mathbf{L} is also sectorial on Z with domain X . Note also that \mathbf{L} has a compact resolvent and thus discrete spectrum accumulating at $-\infty$. We discuss its spectrum in detail in the next section.

3. Spectrum of the linearization. For the bifurcation analysis, we distinguish the stable spectrum of \mathbf{L} , $\sigma_-(\mathbf{L}) := \{\lambda \in \sigma(\mathbf{L}) : \Re(\lambda) < 0\}$, its neutral spectrum $\sigma_0(\mathbf{L}) = \{\lambda \in \sigma(\mathbf{L}) : \Re(\lambda) = 0\}$ and its unstable spectrum $\sigma_+(\mathbf{L}) = \{\lambda \in \sigma(\mathbf{L}) : \Re(\lambda) > 0\}$.

The next Lemma characterizes the spectrum and is the basis for the identification of bifurcations. While this concerns the comoving variable of system (2.1), the spectrum for the original system is the same up to a scaling of the imaginary parts. See §5. Recall that $\ell = L_2/L_1$ is the domain aspect ratio. In the following we set $\mathbb{N}_* = \mathbb{N} \setminus \{0\}$ for clarity.

LEMMA 3.1. *The spectrum $\sigma(\mathbf{L})$ of \mathbf{L} consists of the eigenvalues*

$$\lambda_k^\pm = i\pi \frac{k_2 \Delta T}{\ell L_1} - \pi^2 \frac{\nu_+ + \nu_-}{2L_1^2} \left(k_1^2 + \frac{4k_2^2}{\ell^2} \right) \pm \sqrt{D_k}, \quad k \in \mathbb{N}_* \times \mathbb{Z}, \quad (3.1)$$

where

$$D_k = \frac{k_2^2 \Delta T}{\ell^2 L_1} \left(\frac{4}{k_1^2 + 4(k_2/\ell)^2} - \pi^2 \frac{\Delta T}{L_1} \right) + \mathcal{O}(|\Delta\nu|(k_1^2 + k_2^2)^2). \quad (3.2)$$

In particular, for $0 \leq |\Delta\nu| \ll 1$, $\lambda_k^- \in \sigma_-(\mathbf{L})$, and if $D_k \leq 0$ then $\lambda_k^+ \in \sigma_-(\mathbf{L})$. Moreover, $\Re(\lambda_{(k_1, k_2)}^+) < \Re(\lambda_{(1, k_2)}^+)$.

REMARK 4. *Since $\nu^\pm > 0$ renders \mathbf{L} uniformly elliptic, for fixed $\nu^\pm > 0$ only a bounded set of k can give λ_k^\pm with real part larger than a fixed value, for instance -1 . For $0 \leq |\Delta\nu| \ll 1$ continuity thus gives uniform bounds on the difference to $\Delta\nu = 0$ for critical eigenvalues. Hence, for the considerations of this section, the perturbations are all of order $|\Delta\nu|$ (or higher) with constants uniform in k .*

We will start to discuss the relevance and implications of Lemma 3.1 after its proof. In preparation of the proof, choose the orthogonal basis of X given by

$$g_k(x) := \sin\left(\frac{k_1 \pi x_1}{L_1}\right) \exp\left(\frac{2i\pi k_2 x_2}{L_2}\right), \quad (3.3)$$

where $k \in \mathbb{N}_* \times \mathbb{Z}$. In order to express the operator A , denote

$$\phi_k(x) := \cos\left(\frac{k_1 \pi x_1}{L_1}\right) \exp\left(\frac{2i\pi k_2 x_2}{L_2}\right). \quad (3.4)$$

Indeed, if $f \in X$, the explicit solution to the Poisson equation $-\nabla^2 V = f$ in terms of this basis reads

$$V(x) = \frac{2}{\pi^2} \sum_{k \in \mathbb{N}_* \times \mathbb{Z}} \frac{1}{\frac{L_2}{L_1} k_1^2 + 4 \frac{L_1}{L_2} k_2^2} \left(\int_{\Omega} f(y) \overline{g_k(y)} dy \right) g_k(x).$$

We therefore get the explicit formula for A :

$$Af(x) = -\frac{2}{\pi} \sum_{k \in \mathbb{N}_* \times \mathbb{Z}} \langle f, g_k \rangle \left(\frac{L_2}{L_1} k_1^2 + \frac{4L_1}{L_2} k_2^2 \right)^{-1} \begin{pmatrix} k_1 \phi_k(x)/L_1 \\ 2ik_2 g_k(x)/L_2 \end{pmatrix}. \quad (3.5)$$

Proof. [Lemma 3.1] Consider functions of the form $qg_k(x)$, $k \in \mathbb{N}_* \times \mathbb{Z}$, where $q \in \mathbb{C}^2$ is an arbitrary constant vector. Since

$$A_2 g_k(x) = -\frac{2L_1 i}{\pi} \frac{k_2}{\frac{L_2}{L_1} k_1^2 + 4 \frac{L_1}{L_2} k_2^2} g_k(x), \quad (3.6)$$

the action of \mathbf{L} on such functions is

$$(\mathbf{L}qg_k)(x) = M_k qg_k(x), \quad (3.7)$$

where

$$M_k := \begin{pmatrix} C_1(k)\Delta T - C_2(k) - \nu_- C_3(k) & -C_2(k) \\ C_2(k) & C_2(k) - \nu_+ C_3(k) \end{pmatrix}, \quad (3.8)$$

with

$$C_1(k) := \frac{2\pi k_2 i}{L_2}, \quad C_2(k) := \frac{2i}{\pi} \frac{k_2}{\frac{L_2}{L_1} k_1^2 + \frac{4L_1}{L_2} k_2^2}, \quad C_3(k) := \pi^2 \left(\frac{k_1^2}{L_1^2} + \frac{4k_2^2}{L_2^2} \right).$$

The eigenvalues of M_k are readily computed to be λ_k^\pm . Taking Remark 4 into account, the claims on the real parts of λ_k^\pm immediately follow from inspecting (3.1) for $\Delta\nu = 0$ – in particular D_k monotonically decreases in k_1 . \square

Note that the proof also implies that eigenfunctions of \mathbf{L} have the form

$$\zeta_k(x) := \xi_k g_k(x) \in Z \times Z, \quad (3.9)$$

with ξ_k a eigenvector of M_k .

The last statement in Lemma 3.1 means that, for $0 \leq \Delta\nu \ll 1$, only $D_k > 0$ and $\lambda_{(1,k_2)}^+$ with $k_2 \in \mathbb{Z} \setminus \{0\}$ allow for destabilization, and the real part in this case is (up to terms of order $\Delta\nu$) given by

$$\Re\left(\lambda_{(1,k_2)}^+\right) = -\pi^2 \frac{\nu}{L_1^2} \left(1 + \frac{4k_2^2}{\ell^2}\right) + \sqrt{\frac{k_2^2 \Delta T}{\ell^2 L_1} \left(\frac{4}{1 + 4(k_2/\ell)^2} - \pi^2 \frac{\Delta T}{L_1}\right)}. \quad (3.10)$$

Note that this is a function of the three parameters ν/L_1^2 , $\Delta T/L_1$, $(k_2/\ell)^2$. As expected, increasing viscosity always stabilizes, with increasing impact for increasing $(k_2/\ell)^2$. However, the dependence of the real part on k_2/ℓ is not necessarily monotone, which allows for intricate destabilization scenarios.

The imaginary part, $\Im(\lambda_{(1,k_2)}^+)$, is non-zero unless $\Delta T = 0$, which means that all bifurcations are non-stationary in the reference frame of (2.1) and typically that of (1.1) so that we generically expect Andronov-Hopf bifurcations, where k_2 determines the wavenumber of bifurcating solutions.

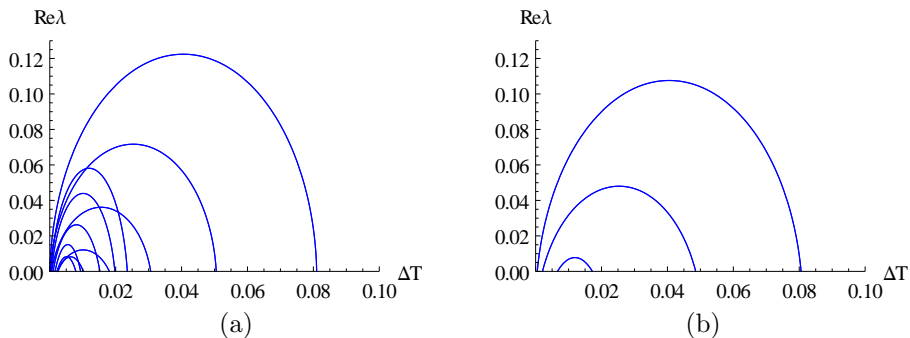


FIG. 3.1. Real parts of eigenvalues as functions of ΔT for $L_1 = L_2 = 1$ and $\Delta\nu = 0$. The unstable eigenvalues with $k \in \{1, \dots, 10\} \times \{-10, \dots, 10\}$ are plotted for (a) $\nu = 10^{-3}$, (b) $\nu = 4 \cdot 10^{-3}$. Eigenmodes with higher wavenumber have smaller ΔT -value of maxima in order. The figure illustrates that linear instabilities occur in a finite interval for ΔT , that in this parameter regime eigenmodes with wavenumber 1 are most unstable, and that increasing ν stabilizes the spectrum globally in ΔT .

Taking the temperature difference ΔT as the primary bifurcation parameter, we next focus on the location of instabilities as ΔT varies, as well as on the wavenumber of destabilizing modes determined by k_2 . In Figure 3.1 we plot sample computations of spectrum as ΔT varies, illustrating the stabilizing effect of the viscosity. Crossings of eigenvalue curves at zero real part can occur, which is expected to generate rich bifurcations. However, in this paper we focus on simple bifurcations.

Recall the spectral conditions at a primary Andronov-Hopf bifurcation

$$\begin{aligned} \text{(i)} \quad & \text{There is a constant } \gamma > 0 \text{ s.t. } \sup\{\Re(\lambda) : \lambda \in \sigma_-(\mathbf{L})\} < -\gamma, \\ \text{(ii)} \quad & \sigma_0(\mathbf{L}) = \{\pm i\omega\}, \omega > 0 \text{ and } \pm i\omega \text{ are simple eigenvalues,} \\ \text{(iii)} \quad & \sigma_+(\mathbf{L}) = \emptyset, \end{aligned} \tag{3.11}$$

and in the nondegenerate case, the critical eigenvalues transversely cross the imaginary axis upon parameter variation.

It turns out that we can characterize a large part of parameter space, where critical eigenvalues have $k_2 = 1$, that is, $k = k_c := (1, 1)$. We therefore define the following particular case of (3.11).

CONDITION 1. *It holds that $\Re(\lambda_{k_c}^+) = \Re(\lambda_{\bar{k}_c}^+) = 0$ and there is $\gamma > 0$ such that $\Re(\lambda_k^\pm) < -\gamma$ for $k \in \mathbb{N}_* \times \mathbb{Z} \setminus \{k_c, \bar{k}_c\}$.*

Here and in the following we denote $\bar{\kappa} = (\kappa_1, -\kappa_2)$ for $\kappa \in \mathbb{R}^2$.

For the remainder of this section we fix $\Delta\nu = 0$ since as before all quantities are smooth in $\Delta\nu$ at $\Delta\nu = 0$, and in the relevant range this is uniform in k , cf. Remark 4.

Rearranging sign conditions on (3.10) and squaring, we readily compute that the sign of $\Re(\lambda_{(1, k_2)}^+)$, for $\kappa_2 = k_2^2$ is the sign of

$$d(\Delta T, \kappa_2) = \frac{4L_1^3}{4\kappa_2 + \ell^2} \Delta T - \frac{L_1^2 \pi^2}{\ell^2} \Delta T^2 - \nu^2 \pi^4 \frac{(4\kappa_2 + \ell^2)^2}{\kappa_2 \ell^4}, \tag{3.12}$$

which is somewhat simpler to handle. In particular, zeros of d are the critical eigenvalues for bifurcations. This yields the following a priori bounds on ΔT for linear instability. Recall $\Delta T_* = \frac{4L_1}{\pi^2}$ for $\Delta\nu = 0$.

LEMMA 3.2. *For all ν, ℓ and $\kappa_2 > 0$, the real roots of $d(\cdot, \kappa_2)$ lie in $(0, \Delta T_*)$. Moreover, the real roots approach the endpoints in the limit $\ell \rightarrow \infty$ if $\nu = o(\ell^{-1})$.*

Proof. Since $d(0, \kappa_2) \leq 0$ and $\partial_{\Delta T} d(0, \kappa_2) > 0$ the lower bound holds. For the upper bound, observe that $d(4L_1/\pi^2, \kappa_2) < 0$ and $\partial_{\Delta T} d(4L_1/\pi^2, \kappa_2) < 0$, which proves the claim since the quadratic coefficient of ΔT is negative. The statement on the limits readily follows from (3.12) upon multiplication by ℓ^2 . \square

Note that $d(\cdot, \kappa_2)$, as a quadratic polynomial in ΔT , has two real roots $\Delta T_1(\kappa_2) \leq \Delta T_2(\kappa_2)$ if and only if the viscosity is sufficiently small,

$$\nu \leq \nu_{\text{crit}}(\kappa_2) := \frac{2\sqrt{\kappa_2} \ell^3 L_1^2}{(4\kappa_2 + \ell^2)^2 \pi^3}, \tag{3.13}$$

with a double root at equality. Hence, this is a necessary and sufficient condition for the occurrence of critical eigenvalues $\lambda_{(1, \sqrt{\kappa_2})}^+$ as ΔT varies. However, it is subtle to determine when the critical eigenvalues destabilize the equilibrium as this requires to exclude unstable eigenvalues for all other k_2 .

Nevertheless, the location of these parabola's maxima in ΔT is at

$$\Delta T = \frac{2\ell^2 L_1}{(4\kappa_2 + \ell^2)\pi^2}, \quad (3.14)$$

which is strictly decreasing in κ_2 . Therefore, the k_2 -value of these parabola in ΔT can be identified by the relative location of their maxima.

REMARK 5. From (3.13) we infer that for fixed $\nu > 0$, increasing aspect ratio ℓ implies increasing wavenumber k_2 ($k_2^2 = \kappa_2$). Specifically, for fixed L_2 and $L_1 \rightarrow 0$ satisfying (3.13) requires that $k_2 = \mathcal{O}(L_1^{-3})$. For fixed L_1 and $L_2 \rightarrow \infty$, the requirement is $k_2 = \mathcal{O}(L_2)$. Concerning the upper destabilization threshold ΔT_2 , it then follows from (3.14) that in the first case $\Delta T_2 = \mathcal{O}(L_1^5)$, while in the second case $\Delta T_2 \rightarrow \Delta T_* = 4L_1/\pi^2$ as $L_2 \rightarrow \infty$ in accordance with Lemma 3.2.

REMARK 6. For $\kappa_2 = 1$ the roots satisfy $\Delta T_1 = \mathcal{O}(\nu^2)$ and $\Delta T_2 = \frac{4\ell^2 L_1}{\pi^2(\ell^2+4)} + \mathcal{O}(\nu^2)$, which was already illustrated in Figure 1.1.

The geometric nature of bifurcating solutions is determined by the k_2 -value of critical and destabilizing eigenvalues as ΔT in- or decreases from outside $[0, \Delta T_*]$. We thus define

DEFINITION 3.3. For given L_1, ℓ, ν , we say that \mathbf{L} possesses a k_2 -instability region, if $d(\cdot, k_2)$ has two positive roots $\Delta T_1(k_2^2) \leq \Delta T_2(k_2^2)$. We call a k_2 -instability region locally primary, if there is a neighbourhood $S \subseteq \mathbb{R}$ of $J := (\Delta T_1(k_2^2), \Delta T_2(k_2^2))$, s.t. the steady state $u = 0$ is stable for $\Delta T \in S \setminus J$ and $\Delta T_j(k_2^2) \neq \Delta T_j(\kappa_2)$ for $\kappa_2 \neq k_2^2$, $j = 1, 2$. Moreover, we say that the k_2 -instability region is primary, if it is locally primary and $S = \mathbb{R}$.

To ease notation, we simply write ΔT_j for $\Delta T_j(1)$, $j = 1, 2$.

As a first step to understand the nature of destabilizing k_2 -instability regions, we consider the case $k_2 = 1$ and in preparation define the following condition.

CONDITION 2. For some given $L_1, \ell, \nu > 0$ we have

$$\frac{\Delta T}{\nu^2 \pi^4} > \frac{(4 + \ell^2)(4k_2^2 + \ell^2)}{16\ell^4 L_1^3 k_2^2} (\ell^4 - 16k_2^2) \quad (3.15)$$

and $\nu < \nu_{crit}(1)$ for $\Delta T \in \{\Delta T_1, \Delta T_2\}$, and all $k_2 \in \mathbb{N}_*$, $k_2 \geq 2$. Note that Condition 2 requires a ratio of threshold temperature difference and viscosity to dominate a ratio involving domain geometry and linear mode harmonics.

THEOREM 3.4.

1. A 1-instability region of \mathbf{L} is locally primary if and only if Condition 2 holds. If it holds, then Condition 1 is satisfied at $\Delta T = \Delta T_j$, $j = 1, 2$. The critical eigenvalues are $\lambda_j = \pm i\omega_j$ with $\omega_j = \pi\Delta T_j/(\ell L_1)$.
2. For $0 < \ell \leq 2\sqrt{2} \approx 2.8$ any 1-instability region of \mathbf{L} is primary and Condition 1 is satisfied at $\Delta T = \Delta T_j$, $j = 1, 2$.

The point of the theorem is that it provides conditions under which the destabilizing mode for increasing and decreasing ΔT is known, namely the lowest spatial harmonic. Note the bound on ℓ in item 2 is not sharp, but it in particular includes the case $\ell = 1$ considered in [10].

Proof.

1. A direct calculation gives

$$\frac{d(\Delta T, 1) - d(\Delta T, \kappa_2)}{\kappa_2 - 1} = \frac{16\Delta T \kappa_2 \ell^4 L_1^3 - (4 + \ell^2)(4\kappa_2 + \ell^2)(\ell^4 - 16\kappa_2)\nu^2 \pi^4}{\kappa_2 \ell^4 (4 + \ell^2)(4\kappa_2 + \ell^2)}. \quad (3.16)$$

In particular, Condition 2 is indeed equivalent to a 1-instability region being locally primary. The claims on ΔT follow readily from inspection of the zeros of d .

2. This is the trivial observation that the right hand side in condition 3.15 is strictly negative for these values of ℓ , while the left hand side is positive at all possible real roots ΔT of $d(\cdot, \kappa_2)$ on account of Lemma 3.2.

□

REMARK 7. *The critical frequencies in the original x_2 -variable of (1.1) are*

$$\omega_j = (T_j^+ + T_j^-) \frac{\pi}{L_2}.$$

The following corollary guarantees that other destabilization scenarios also occur.

COROLLARY 3.5. *Let $\kappa_2 > 1$ and let ℓ be the unique positive solution $\ell = \ell_{\kappa_2}$ of*

$$\ell^6 - \kappa_2 \ell^4 - 80\kappa_2 \ell^2 - 64\kappa_2(2 + \kappa_2) = 0. \quad (3.17)$$

Then for $\nu = \nu_{\text{crit}}(1)$ the 1-instability region is a point, $\Delta T_1 = \Delta T_2$, that coincides with $\Delta T_2(\kappa_2)$. Notably, ℓ_{κ_2} is strictly increasing in κ_2 .

Proof. Substituting the critical $\nu^2 = \frac{4\ell^6 L_1^4}{(4+\ell^2)^4 \pi^6}$ from (3.13) and the corresponding critical value of $\Delta T = \frac{2\ell^2 L_1}{\pi^2(4+\ell^2)}$ at the double root into the nominator of the right hand side of (3.16) gives

$$\frac{4\ell^6 L_1^4}{(4 + \ell^2)^3 \pi^2} (64\kappa_2(2 + \kappa_2) + 80\kappa_2 \ell^2 + 4\kappa_2 \ell^4 - \ell^6),$$

where $\kappa_2 = k_2^2$. The first factor is positive and roots of the second factor, which we denote by q , precisely solve (3.17). We have

$$\partial_{(\ell^2)} q = 80\kappa_2 + 8\kappa_2 \ell^2 - 3\ell^4,$$

which is positive at $\ell = 0$ so that the cubic q with negative cubic coefficient has a unique positive root. In addition, this implies that $\partial_{\ell} q < 0$ at this root so that together with

$$\partial_{\kappa_2} q = 4(32 + 32\kappa_2 + 20\ell^2 + \ell^4) > 0$$

we infer from implicit differentiation that the location of this root strictly increases with κ_2 . □

This means that the 1-instability region is not primary. In fact, it is also not primary for nearby parameter values that produce $\Delta T_2(4) > \Delta T_2(1)$. The solution to (3.17) for $\kappa_2 = 4$ is $\ell_4 \approx 5.37$, and for $\kappa_2 = 9$ it is $\ell_9 \approx 7.22$. See Figure 3.2. For ℓ between these values (and slightly above ℓ_9), we numerically find that the 2-instability region is primary. In general, for any given k_2 Condition 2 is violated for sufficiently large ℓ (with ν, L_1 fixed), since ΔT is bounded (Lemma 3.2).

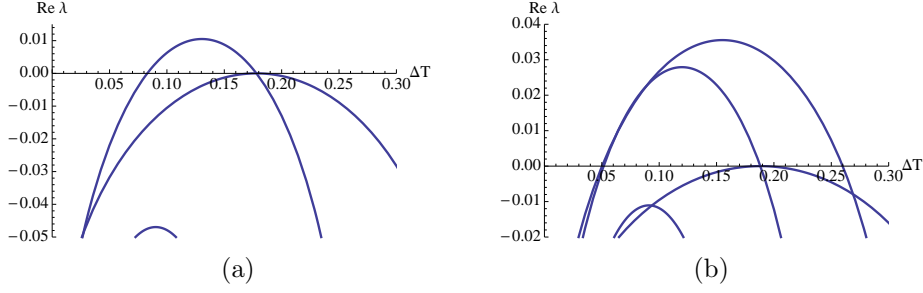


FIG. 3.2. Real parts of eigenvalues λ_k^+ , $k = (1, k_2)$, as functions of ΔT for $\Delta\nu = 0$. The parabola are ordered in k_2 by the decreasing location of maxima. Here $\nu = \nu_{\text{crit}}(1)$ so that $\Delta T_1 = \Delta T_2$. (a) $\ell = \ell_4$, with near primary 2-instability region. (b) $\ell = \ell_9$, with primary 2-instability region.

REMARK 8. It is possible to show that for ν small enough, there is a primary 1-instability region, if $\ell < \ell^* \approx 4.053$, where ℓ^* is the unique positive root of the polynomial $16(\ell^2 + 4)^2 - (\ell^2 - 8)(\ell^2 + 8)(\ell^2 + 16) = 0$.

For the case of small viscosity, we have the following corollary of Theorem 3.4.

COROLLARY 3.6. As $\nu \rightarrow 0$, \mathbf{L} has k_2 -instability regions for $k_2 \rightarrow \infty$ with $\Delta T_1(k_2^2) < \Delta T_2(k_2^2)$. For sufficiently small ν , Condition 1 is satisfied at $\Delta T_2(1)$, and this is an instability threshold.

Proof. The presence of all k_2 -instability regions clearly holds at $\nu = 0$ in view of (3.13). In addition, from (3.16) we infer at $\nu = 0$ that

$$d(\Delta T, 1) - d(\Delta T, \kappa_2) > 0,$$

so that the critical eigenfunction at the right endpoint of the instability interval has mode number $k_2 = \pm 1$. This persists for sufficiently small $\nu > 0$, since the thresholds depend continuously on ν , and again from 3.16 we see that for each $\nu > 0$ there is only a finite range of κ_2 values, for which $d(\Delta T, 1) - d(\Delta T, \kappa_2) < 0$ is possible. \square

Lastly, we point out the possibility of multiple disjoint primary k_2 -instability regions, where changing ΔT destabilizes and stabilizes multiple times. The following lemma shows that there can be at most two such regions since $\kappa = k_2^2$ is discrete. On the infinite strip the lemma implies a Turing-type instability, see Lemma 5.1 in §5 below.

LEMMA 3.7. Fix L_1, L_2, ν and consider $d(\Delta T, \kappa)$ as map $d: \mathbb{R} \times \mathbb{R}^+ \rightarrow \mathbb{R}$. Then d has a unique critical point, which is a global maximum $(\Delta T_{\text{max}}, \kappa_{\text{max}})$ with $\kappa_{\text{max}} > 0$ and $\partial_\kappa^2 d(\Delta T_{\text{max}}, \kappa_{\text{max}}) < 0$. Moreover, for any ΔT , the function $d(\Delta T, \cdot)$ has a unique positive maximum.

Proof. For fixed ΔT we compute

$$\partial_\kappa^2 d(\Delta T, \kappa) = \frac{2^7 L_1^3 \Delta T}{(4\kappa + \ell^2)^3} - \frac{2\nu^2 \pi^2}{\kappa^3}$$

so that a change in convexity (in κ -direction) for $\kappa > 0$ requires

$$4(L_1 \Delta T^{(1/3)} - \nu^2 \pi^2) \kappa = \ell^2,$$

which has at most one solution. Since $d(\Delta T, \kappa)$ as a function of κ is convex near $\kappa = 0$ and $d(\Delta T, \kappa) \rightarrow -\infty$ as $\kappa \rightarrow \infty$, this implies a unique critical point in the convex region, which is therefore a global maximum for $\kappa > 0$.

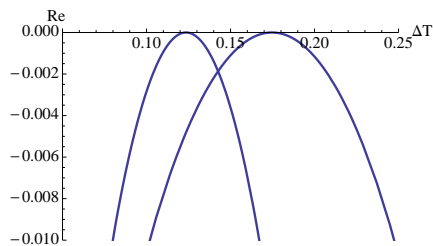


FIG. 3.3. Real parts of eigenvalues λ_k^+ , $k = (1, k_2)$, as functions of ΔT for $\Delta\nu = 0$. Here $\ell = 2\sqrt{2} + 3\sqrt{2}$ so that $\nu_{\text{crit}}(1) = \nu_{\text{crit}}(4)$. In the plotted region only the curves with $k_2 = 1, 4$ are present. This illustrates the possibility of k_2 -instability regions with $k_2 > 1$, that is, the onset can come through higher harmonics in x_2 -direction.

Putting this together with the fact that $d(\Delta T, \kappa)$ is a convex quadratic polynomial in ΔT we infer the lemma statement. \square

In Figure 3.3 we plot eigenvalue curves, where two k_2 -instability regions consist of a point. Parameters $\nu = \nu_{\text{crit}}(k_2) = \nu_{\text{crit}}(k'_2)$ and ℓ that produce such scenarios can be readily computed from (3.13); here we take $k_2 = 1$, $k'_2 = 4$. For perturbed $\nu < \nu_{\text{crit}}(1)$ the instability regions become disjoint open intervals.

REMARK 9. On account of (3.13), for decreasing ν and also for increasing ℓ , there is an increasingly long sequence of secondary instabilities of Andronov-Hopf type as ΔT increases from zero, with higher and higher spatial harmonics, and another reverse sequence as ΔT is moved towards ΔT_* . See Figure 3.1.

4. Center manifold reduction. In this section, we consider the vicinity of parameters with critical $\Delta T = \Delta T_j$ for $j = 1$ or $j = 2$ and assume that no other eigenvalues lies on the imaginary axis. The main example is a primary 1-instability region. For the unfolding of the bifurcation in the generic case $\Delta T_1 < \Delta T_2$ we introduce the parameter μ_1 by $\Delta T = \Delta T_j + \mu_1$. In the degenerate case $\Delta T_1 = \Delta T_2$, where $\nu = \nu_{\text{crit}}(1)$, we additionally unfold with μ_2 defined by $\nu = \nu_{\text{crit}}(1) - \mu_2^2$ and perturb from $\Delta\nu = 0$ to highlight the effect of symmetry breaking, cf. Remark 1. For readability we frequently suppress the index j .

At bifurcation, the critical eigenvalues are then $\pm i\omega$ and we denote the associated eigenfunctions by $\zeta(x) := \zeta_{k_c}(x)$, $\bar{\zeta}(x)$, see (3.9). Then \mathbf{L} possesses a two-dimensional real central subspace $E_c := \text{span}\{\Re(\zeta), \Im(\zeta)\} \subset Z^2$ and we will show that there is a locally invariant 2D center manifold

$$W_c = \{u_0 + \psi(u_0, \mu) : u_0 \in O_{E_c}\} \subset O_{Z^2}, \mu \in O_{\mathbb{R}^2},$$

with $\psi : O_{E_c} \rightarrow E_c^\sharp$, $E_c \oplus E_c^\sharp = Z^2$, and neighbourhoods $O_{\mathbb{R}^2}$ of $\mu = 0$, and O_{E_c} , O_{Z^2} of $0 \in Z^2$. In case of a primary bifurcation the center manifold is also locally exponentially attracting.

Since we consider $k = k_c = (1, 1)$, it is not surprising that the coefficients $C_m(k_c)$ defined in (3.8) show up. It turns out that following modifications are convenient.

$$c_1 := \frac{\pi\Delta T}{L_2}, \quad c_2 := \frac{2}{\pi\left(\frac{L_2}{L_1} + \frac{4L_1}{L_2}\right)}, \quad c_3 := \nu\pi^2\left(\frac{1}{L_1^2} + \frac{4}{L_2^2}\right). \quad (4.1)$$

We give an overview of the main results in this section and postpone the lengthy proofs of Theorem 4.1, Corollary 4.2 and Theorem 4.3 to §4.1. First consider the

generic case of (3.13), where the unfolding goes by μ_1 only. See Fig. 1.1 for a partial illustration.

THEOREM 4.1. *Suppose that Condition 1 holds for a fixed parameter set for which $\Delta T_1 < \Delta T_2$. Then the steady state $u = 0$ of system (2.5) possesses a locally exponentially attracting and locally invariant 2D center manifold near $u = 0$ with the normal form dynamics of $z = re^{i\varphi}$ given by*

$$\begin{aligned}\frac{dr}{dt} &= \mu_1 a_1 r + br^3 + \mathcal{O}(r(|\mu_1| + r^2)^2 + |r\Delta\nu|), \\ \frac{d\varphi}{dt} &= \omega_0 + \mu_1 a_0 + \Delta\nu \tilde{b} r^2 + \mathcal{O}(|\Delta\nu| + \Delta\nu^2 r^2),\end{aligned}\tag{4.2}$$

where

$$a_1 = \frac{\pi}{L_2} \frac{c_2 - c_1}{c_3}, \quad b = -\frac{L_1^4}{4\pi^2\nu} \frac{c_1^2 + c_3^2}{L_2^2 + 4L_1^2}, \quad \omega_0 = \frac{\pi\Delta T}{L_2}, \quad a_0 = \frac{\pi}{L_2},\tag{4.3}$$

$$\tilde{b} = \frac{c_3 L_1^3 L_2}{(L_2^2 + 4L_1^2)^2} \left(\frac{c_2^2}{2c_2 - c_1} + \frac{L_2^2 + 4L_1^2}{L_2^2} (2c_1 - c_2) \right)\tag{4.4}$$

The following corollary highlights the nature of the resulting bifurcations. The relation to travelling waves mentioned in Remark 1 will be made explicit in §5.

COROLLARY 4.2. *Assume the hypotheses of Theorem 4.1. Then the steady state $u = 0$ of (2.5) undergoes a supercritical Andronov-Hopf bifurcation as μ_1 varies. The reduced vector field coefficients satisfy $b < 0$, $\text{sgn}(a_1) = -(-1)^j$ at $\Delta T = \Delta T_j$ and $\tilde{b} \neq 0$ at ΔT_2 and if $\ell > 2$ also at ΔT_1 ; otherwise generically $\tilde{b} \neq 0$. In particular, near the stability thresholds there exist heteroclinic connections between the unstable steady state and the stable limit cycle.*

As $\nu \downarrow 0$, the radius of the limit cycles scales near ΔT_1 as $r(t) \propto \nu^{-1} \sqrt{\Delta T - \Delta T_1}$, and near ΔT_2 as $r(t) \propto \sqrt{\Delta T_2 - \Delta T}$.

Next, we formulate the result for unfolding the codimension-2 case $\Delta T_1 = \Delta T_2$, where the critical eigenvalues do not transversely cross the imaginary axis.

THEOREM 4.3. *Suppose that Condition 1 holds for a fixed parameter set for which $\Delta T_1 = \Delta T_2$. Then the steady state $u = 0$ of system (2.5) possesses a locally exponentially attracting and locally invariant 2D center manifold near $u = 0$ with the normal form dynamics for $z = re^{i\varphi}$ given by $\frac{dz}{dt}$ as in Theorem 4.1 and*

$$\begin{aligned}\frac{dr}{dt} &= a_1 \mu_1 (a_2 \mu_2 - a_3 \mu_1) r + br^3 + \mathcal{R}, \\ \mathcal{R} &= \mathcal{O}(\mu_2^2 + |\mu_1 \mu_2^3| + r(|\mu| + r^2)^2 + |r\Delta\nu|), \quad \text{with} \\ a_0 &= \frac{\pi}{L_2}, \quad a_1 = \frac{\pi^2}{L_2^2}, \quad a_2 = \frac{1}{\sqrt{\pi} L_1 L_2}, \quad a_3 = \frac{\pi}{L_2^2},\end{aligned}\tag{4.5}$$

and b from Theorem 4.1.

In particular, for $0 \leq |\Delta\nu| \ll |\mu_2| \ll 1$, there exists a branch of stable periodic orbits, parametrized by μ_1 and terminating at supercritical Andronov-Hopf bifurcations at $\Delta T + \mu_1 = \Delta T_j$, $j = 1, 2$.

The following Theorem shows that the bifurcation results 4.1-4.3 can be generalized to instabilities caused by higher spatial harmonics.

THEOREM 4.4. *Assume (3.11) holds with critical wavenumber k_2 , so that $\lambda_{(1,k_2)}^+ = i\omega$. If $\Delta T_1(k_2^2) < \Delta T_2(k_2^2)$ then the statements of Theorem 4.1 and Corollary 4.2 hold*

with ΔT_j replaced by $\Delta T_j(k_2^2)$, and L_2 replaced by L_2/k_2 for the coefficients on the center manifold. If $\Delta T_1(k_2^2) = \Delta T_2(k_2^2)$ then the statement of Theorem 4.3 holds for the same modifications.

Proof. Under condition (3.11) the center manifold theorem applies as in the first parts of the proofs of Theorems 4.1 and 4.3. This yields a stable locally invariant manifold with reduced dynamics of Hopf normal form (with the frequency independent of amplitude for $\Delta\nu = 0$). The only remaining question is the sign of the coefficients.

If k_2 is the critical wavenumber in x_2 -direction on the domain $[0, L_1] \times [0, L_2]$ then 1 is this wavenumber on the domain $[0, L_1] \times [0, L_2/k_2]$ so that Condition 1 holds there. Hence, on this domain and with the modifications in the claim, Theorem 4.1, Corollary 4.2 and Theorem 4.3 hold fully.

The theorem now follows since the bifurcating branches imbed into the original domain. \square

REMARK 10. *Recall that there is a sequence of secondary instabilities as noted in Remark 9. Whenever these occur with a simple pair of complex conjugate eigenvalues, analogous center manifold reduction results hold for an unstable 2D manifold. The reduced vector fields are of the same form with coefficients given analogous to the above results, but to be computed at different k_2 and other parameters.*

4.1. Proofs of Theorem 4.1, Corollary 4.2 and Theorem 4.3.

Proof. [Theorem 4.1] For the unfolding with μ_1 , we modify the definition of R in (2.5) by adding the term $\mu_1 \partial_{x_2} u_1$ in the first component and denote the result by $R(u; \mu_1)$. For the resulting bifurcation problem, we verify the hypotheses of the center manifold theorem [12, Theorem 3.3, p.46]. We will employ the $O(2)$ -symmetry for $\Delta\nu = 0$ noted in Remark 1 only at the end to highlight the steady state nature of the bifurcations. The goal now is the full justification of the center manifold reduction and the computations of the coefficients on the center manifold independent of an additional symmetry.

As noted after (2.5), $\mathbf{L} \in \mathcal{L}(Z^2, X^2)$ is sectorial so that Hypothesis 2.7 in that theorem holds, using [12, Remark 2.18 p. 37]. Hypotheses 3.1(i) and 2.4 hold on account of Theorem 3.4. It remains to show Hypotheses 3.1(ii): smoothness of R . From (2.5) we explicitly compute

$$DR(u; \mu_1)v = \begin{pmatrix} \mu_1 \partial_{x_2} v_1 - A^\perp(v_1 + v_2) \cdot \nabla u_1 - A^\perp(u_1 + u_2) \cdot \nabla v_1 \\ -A^\perp(v_1 + v_2) \cdot \nabla u_2 - A^\perp(u_1 + u_2) \cdot \nabla v_2 \end{pmatrix},$$

$$D^2R(u; \mu_1)[v, w] = - \begin{pmatrix} A^\perp(v_1 + v_2) \cdot \nabla w_1 + A^\perp(w_1 + w_2) \cdot \nabla v_1 \\ A^\perp(v_1 + v_2) \cdot \nabla w_2 + A^\perp(w_1 + w_2) \cdot \nabla v_2 \end{pmatrix}.$$

Note that $A^\perp(v_1 + v_2) \in \mathbf{H}^3 \times \mathbf{H}^3$ and $\nabla w \in \mathbf{H}^2 \times \mathbf{H}^2$. Since \mathbf{H}^2 is a Banach algebra (see for instance [1, Theorem (4.39)]), there is a constant $C_0 > 0$, such that

$$\|A^\perp(v_1 + v_2) \cdot \nabla w\|_{\mathbf{H}^2} \leq C_0 \|A^\perp(v_1 + v_2)\|_{\mathbf{H}^2 \times \mathbf{H}^2} \|\nabla w\|_{\mathbf{H}^2 \times \mathbf{H}^2}.$$

Also $A^\perp(v_1 + v_2) \cdot \nabla w$ vanishes at $x_1 = 0, L_1$, hence $\|D^2R(u; \mu_1)[v, w]\|_{Y^2} \leq C \|v\|_{Z^2} \|w\|_{Z^2}$, that is, $R(u; \mu_1) \in C^2(Z^2, Y^2)$. Moreover all the higher derivatives are identically 0, hence R is analytic. This establishes the existence of the 2D center manifold and smoothness of ψ as needed below, and for which the reduced dynamics has the normal form (4.2). Here the critical frequency is $\omega = \pi \Delta T / L_2 + \mathcal{O}(\Delta\nu)$ due to Theorem 3.4. In order to analyze the coefficients of the reduced equation, we write functions in the central subspace as

$$u_0(t) = z(t)\zeta + \overline{z(t)\zeta}, \quad z(t) \in \mathbb{C}.$$

Using the expressions in [12, p. 125] we have for $a = a_1 + ia_0$,

$$a = \langle R_{11}(\zeta) + 2R_{20}(\zeta, \psi_{001}), \zeta^* \rangle_2, \quad (4.6)$$

$$\beta = \langle 2R_{20}(\zeta, \psi_{110}) + 2R_{20}(\bar{\zeta}, \psi_{200}) + 3R_{30}(\zeta, \zeta, \bar{\zeta}), \zeta^* \rangle_2, \quad (4.7)$$

with β the complex cubic coefficient on the center manifold so that $b = \Re(\beta)$ and $\tilde{b} = \frac{d}{d\Delta\nu}\Im(\beta)$ both evaluated at $\Delta\nu = 0$. The quantities in these expressions are defined as follows: ζ^* is the adjoint eigenvector to ζ , the operators R_{ik} are given by, see [12, p. 95-96],

$$\begin{aligned} R_{01} &:= \partial_{\mu_1} R(0; 0) = 0, \\ R_{20}[v, w] &:= \frac{1}{2} D^2 R(0; 0)[v, w] \\ &= -\frac{1}{2} \left(A^\perp(v_1 + v_2) \cdot \nabla w_1 + A^\perp(w_1 + w_2) \cdot \nabla v_1 \right) \\ &\quad - \frac{1}{2} \left(A^\perp(v_1 + v_2) \cdot \nabla w_2 + A^\perp(w_1 + w_2) \cdot \nabla v_2 \right), \quad (4.8) \\ R_{11}v &:= \partial_{\mu_1} DR(0; 0)v = \begin{pmatrix} \partial_{x_2} v_1 & 0 \\ 0 & 0 \end{pmatrix}, \\ R_{30} &= \frac{1}{3!} D^3 R = 0, \end{aligned}$$

and the functions ψ_{ijk} , from the expansion of ψ , are the unique solutions to

$$\begin{aligned} -\mathbf{L}\psi_{001} &= R_{01}, \\ (2\omega i - \mathbf{L})\psi_{200} &= R_{20}(\zeta, \zeta), \\ -\mathbf{L}\psi_{110} &= 2R_{20}(\zeta, \bar{\zeta}). \end{aligned} \quad (4.9)$$

Computation of a . Since $R_{01} = 0$ and $\ker(\mathbf{L}) = \{0\}$, $-\mathbf{L}\psi_{001} = R_{01}$ implies $\psi_{001} = 0$. For this result the parameter μ_2 is held fixed at zero so that, using (4.6), the coefficient a of the reduced system (4.2) is

$$a = \langle R_{11}(\zeta), \zeta^* \rangle_2 = \frac{2\pi\xi^1 i}{L_2} \langle (g_{1,1}, 0)^T, \zeta^* \rangle_2, \quad (4.10)$$

where ζ^* is the adjoint eigenfunction, satisfying

$$\mathbf{L}^* \zeta^* = -i\omega \zeta^*, \quad \langle \zeta, \zeta^* \rangle_2 = 1. \quad (4.11)$$

with the adjoint operator of \mathbf{L} given by (using integration by parts)

$$\begin{aligned} \mathbf{L}^* v &= \begin{pmatrix} -\Delta T \partial_{x_2} v_1 + \frac{1}{L_1} Bv + \nu \nabla^2 v_1 \\ \frac{1}{L_1} Bv + (\nu + \Delta\nu) \nabla^2 v_2 \end{pmatrix}, \quad v \in Y_2 \\ Bv(x) &= \frac{4i}{L_2 \pi} \sum_{k \in \mathbb{N}_* \times \mathbb{Z}} \frac{k_2}{\frac{L_2}{L_1} k_1^2 + \frac{4L_1}{L_2} k_2^2} \langle v_1 - v_2, g_k \rangle g_k(x). \end{aligned}$$

The critical adjoint eigenfunction ζ^* , as any eigenfunction of \mathbf{L}^* , has the form $\zeta^*(x) = \eta g_m(x)$, where $\eta = (\eta^1, \eta^2) \in \mathbb{C}^2$ is an eigenvector of M_m^* derived from (3.8). If $m \neq (1, 1)$, then $\langle \zeta, \zeta^* \rangle_2 = 0$, therefore $m = (1, 1)$, and hence $M_{1,1}^* \eta = -i\omega \eta$ so that from $\langle g_{11}, g_{11} \rangle = L_1 L_2 / 2$ and (4.10) we infer

$$a = \pi \xi^1 \bar{\eta}^1 L_1 i. \quad (4.12)$$

Due to (3.7), there is $\xi \in \mathbb{C}^2$ such that

$$M_{1,1}\xi = i\omega\xi, \xi = (\xi^1, \xi^2)^T, \quad (4.13)$$

and using (4.1) at the bifurcation points $\Delta T = \Delta T_j$, $j = 1, 2$, we have

$$c_3^2 = c_1(2c_2 - c_1) + \mathcal{O}(\Delta\nu). \quad (4.14)$$

Putting this together with equation (4.11) we obtain with $\tilde{\nu} = (1 + \nu/\Delta\nu)$ that

$$\begin{aligned} (M_{1,1} - i\omega)\xi &= \begin{pmatrix} c_1i - c_2i - c_3 & -c_2i \\ c_2i & -c_1i + c_2i - \tilde{\nu}c_3 \end{pmatrix} \xi = 0 \\ (M_{1,1}^* + i\omega)\eta &= \begin{pmatrix} -c_1i + c_2i - c_3 & -c_2i \\ c_2i & c_1i - c_2i - \tilde{\nu}c_3 \end{pmatrix} \eta = 0. \end{aligned} \quad (4.15)$$

Since $M_{1,1}$ is semi-simple at the bifurcation point with the eigenvectors $\xi, \bar{\xi}$, we have $\xi \cdot \eta = 0$ and we can choose $\xi = \xi_0 + \Delta\nu\tilde{\xi} + \mathcal{O}(\Delta\nu^2)$, $\nu = \nu_0 + \Delta\nu\tilde{\eta} + \mathcal{O}(\Delta\nu^2)$ so that $\xi \in \text{span}(\bar{\xi}_0)$, $\tilde{\eta} \in \text{span}(\bar{\eta}_0)$. Specifically, we take

$$\begin{aligned} \xi_0 &= \begin{pmatrix} c_2i \\ c_1i - c_2i - c_3 \end{pmatrix}, \bar{\eta}_0 = \delta \begin{pmatrix} -c_2i \\ c_1i - c_2i - c_3 \end{pmatrix}, \\ \tilde{\xi} &= -\frac{i}{2\omega} \begin{pmatrix} c_3 \\ \nu \end{pmatrix} \begin{pmatrix} 0 \\ \xi_0^2 \end{pmatrix} - \tilde{\lambda}\xi_0, \bar{\tilde{\eta}} = \frac{i}{2\omega\delta} \begin{pmatrix} c_3 \\ \nu \end{pmatrix} \begin{pmatrix} 0 \\ \eta_0^2 \end{pmatrix} - \tilde{\lambda}\xi_0, \\ \delta &= \frac{2}{L_1L_2} \frac{1}{(c_1i - c_3)(c_1i - 2c_2i - c_3)} = \frac{c_3 - i(c_2 - c_1)}{L_1L_2c_3c_2^2}. \end{aligned} \quad (4.16)$$

where $\delta \neq 0$ provides a normalization and we used (4.14). In particular,

$$\xi \cdot \bar{\eta} = \frac{2}{L_1L_2} + \mathcal{O}(\Delta\nu^2). \quad (4.17)$$

From (4.12) at $\Delta\nu = 0$ we thus obtain $a_1 + ia_0 = \pi c_2^2 L_1 \delta i$ as claimed.

Computation of b, \tilde{b} . Thanks to (4.13), $\zeta(x) = \xi g_{1,1}(x)$ so that the nonlinearity R has the property $R(\zeta) = R_{20}(\zeta, \zeta) = 0$, cf. Remark 2, and $\ker(2i\omega - \mathbf{L}) = \{0\}$ on account of Theorem 3.4. Hence, the equation for ψ_{200} from (4.9) implies $\psi_{200} = 0$. Together with $R_{30} = 0$ and (4.7), this means

$$\beta = \langle 2R_{20}(\zeta, \psi_{110}), \zeta^* \rangle_2. \quad (4.18)$$

Next, we compute ψ_{110} using (4.9) and that for $k \in \mathbb{N}_* \times \mathbb{Z}$ we have

$$A_1 g_k(x) = -\frac{L_2^2 L_1 k_1}{\pi(L_2^2 k_1^2 + 4L_1^2 k_2^2)} \phi_k(x). \quad (4.19)$$

Using $\zeta = \xi g_{11}$, (2.4), (3.6), (3.5) and (4.19), straightforward calculations give

$$-\mathbf{L}\psi_{110} = 2R_{20}(\zeta, \bar{\zeta}) = \frac{2i}{K_1} (\xi^1 + \xi^2) \bar{\xi} g_{2,0},$$

where $K_1 := \frac{L_2^2}{L_1} + \frac{4L_1}{L_2}$. Since the eigenvectors $(\xi_k g_k)_{k \in \mathbb{N}_* \times \mathbb{Z}}$ of \mathbf{L} are mutually orthogonal and

$$M_{2,0} = -\frac{4\pi^2}{L_1^2} \begin{pmatrix} \nu & 0 \\ 0 & \nu + \Delta\nu \end{pmatrix}$$

we have that $\psi_{110} = \hat{\xi}g_{2,0}$, where

$$\hat{\xi} = \alpha \left(\bar{\xi} - \begin{pmatrix} 0 \\ \Delta\nu\bar{\xi}_2 \end{pmatrix} \right) + \mathcal{O}(\Delta\nu^2), \quad \alpha = \frac{L_1^2 i}{2\pi^2 \nu K_1} (\xi^1 + \xi^2).$$

This readily gives $R_{20}(\zeta, \psi_{110}) = \check{\xi}g_{1,1}\phi_{2,0}$, where

$$\check{\xi} = -2i \left(\frac{\xi^1 + \xi^2}{K_1} \hat{\xi} - \frac{\bar{\xi}^1 + \bar{\xi}^2}{K_2} \xi \right) \quad (4.20)$$

$$(4.21)$$

with $K_2 = 4\frac{L_2}{L_1}$. Substitution into (4.18) and using $\xi \cdot \eta = 0$ yields up to order $\Delta\nu^2$

$$b = \langle 2R_{20}(\zeta, \psi_{110}), \zeta^* \rangle_2 = -L_1 L_2 i \alpha \left(-\frac{\bar{\xi}^1 + \bar{\xi}^2}{K_2} \xi \cdot \bar{\eta} - \Delta\nu \left(\frac{\xi^1 + \xi^2}{K_1} \bar{\xi}^2 \bar{\eta}_2 + \frac{\bar{\xi}^2}{K_2} \xi \cdot \bar{\eta} \right) \right).$$

On the one hand, evaluation at $\Delta\nu = 0$ together with $\xi \cdot \bar{\eta} = \frac{2}{L_1 L_2}$ we obtain

$$b = -\frac{L_1^4}{4\pi^2 \nu} \frac{c_1^2 + c_3^2}{L_2^2 + 4L_1^2}$$

as claimed.

On the other hand, substituting the expansions of ξ, η , using (4.17) and discarding a priori real terms gives

$$\tilde{b} = -\frac{L_1^3 L_2}{2K_1} \Im \left(\frac{(\xi_0^1 + \xi_0^2)}{K_1} \bar{\xi}_0^2 \bar{\eta}_0^2 + \frac{\xi_0^1 + \xi_0^2}{K_2} \bar{\xi}_0^2 \xi_0 \cdot \bar{\eta}_0 \right).$$

Using (4.14) we readily compute

$$\tilde{b} = -c_3 \frac{L_1^2}{K_1} \left(\frac{c_2^2}{K_1(c_1 - 2c_2)} + \frac{c_2 - 2c_1}{K_2} \right),$$

which gives \tilde{b} as claimed.

For $\Delta\nu = 0$ this gives the truncated normal form equation on the center manifold

$$\frac{d}{dt} z = i(\omega + a_0 \mu_1) z + b z |z|^2$$

and it remains to show that $z = r e^{i\varphi}$ has $\frac{d}{dt} \varphi$ independent of the amplitude r . As mentioned before, this results from the reflection symmetry noted in Remark 1, which means we are in the $O(2)$ -symmetric case Theorem 2.18 of [12] ($\omega = 0$ in the reference frame of Remark 1). See also §5. \square

We now turn to the proof of Corollary 4.2.

Proof. [Corollary 4.2] From (4.4) and (4.1) we readily check $b < 0$, and since $c_3 > 0$, the sign of a_1 is the sign of $c_2 - c_1$. Noting that

$$\frac{2\pi}{L_2} (c_2 - c_1) = \partial_{\Delta T} d(\Delta T, 1) / L_1^4, \quad (4.22)$$

and that the quadratic polynomial $d(\cdot, 1)$ has negative quadratic coefficient, it follows that $c_1 < c_2$ at $\Delta T = \Delta T_1$ and so $a_1 > 0$. Similarly, at $\Delta T = \Delta T_2$ we have $c_2 < c_1$, hence $a_1 < 0$.

Concerning \tilde{b} we have $c_1 - 2c_2 < 0$ due to (4.14), and at ΔT_2 it holds $c_2 < c_1$ as noted above. Thus $\tilde{b} < 0$ at ΔT_2 . Rearranging terms gives \tilde{b} up to a positive factor as

$$\frac{K_1 c_1 (5c_2 - 2c_1) + c_2^2 (K_2 - 2K_1)}{c_1 - 2c_2},$$

where $5c_2 - 2c_1 > 0$ due to (4.14) and $K_2 - 2K_1 = 2(\ell - 4/\ell)$ with aspect ratio $\ell = L_2/L_1$. Since $c_1 - 2c_2 < 0$ we thus have $\tilde{b} < 0$ for $\ell > 2$ and generically in ℓ since $c_2 \neq 0$.

In conclusion, supercritical Andronov-Hopf bifurcations occur at both endpoints of the instability region, where the phase dynamics is linear in case $\Delta\nu = 0$ (and possibly at non-generic parameter values at ΔT_1 for $\ell < 2$). As usual, the local invariance of the center manifold from Theorem 4.1 implies the existence of the claimed heteroclinic orbit between the unstable steady state and the stable limit cycle contained in the center manifold.

Now consider the behaviour of a_1 and b for small viscosity $0 < \nu \ll 1$. With $c_4 := \frac{c_3}{\nu}$ we get $c_2, c_4 = \mathcal{O}(1)$, and

$$a = \pi \frac{c_2 - c_1}{L_2 \nu c_4}, \quad b = -\frac{L_1^3}{4\pi^2 \nu} \frac{c_1^2 + \nu^2 c_4^2}{\frac{L_2^2}{L_1} + 4L_1}.$$

Left endpoint of the instability region: ΔT_1 . Using $c_2 > c_1$ and (4.14) we find $c_1 = c_2 - \sqrt{c_2^2 - \nu^2 c_4^2}$, where $c_2^2 - \nu^2 c_4^2 > 0$ by (3.13). Hence,

$$c_1 = \frac{c_4^2}{2c_2^2} \nu^2 + \mathcal{O}(\nu^4),$$

and we obtain

$$a = \frac{\pi c_2}{L_2 c_4} \frac{1}{\nu} + \mathcal{O}(\nu), \quad b = -\frac{L_1^4 c_4^2}{4\pi^2 (4L_1^2 + L_2^2)} \nu + \mathcal{O}(\nu^3).$$

Therefore the radius of the stable limit cycle $|z(t)|$ for sufficiently small μ_1 is

$$\frac{2\pi}{L_1^2 c_4} \left(\frac{\pi (4L_1^2 + L_2^2) c_2}{L_2 c_4} \right)^{\frac{1}{2}} \frac{1}{\nu} \mu_1^{\frac{1}{2}} + \mathcal{O}(\nu^{\frac{1}{2}}).$$

Right endpoint of the instability region: ΔT_2 . Here $c_1 = c_2 + \sqrt{c_2^2 - \nu^2 c_4^2}$, therefore $c_1 = 2c_2 + \mathcal{O}(\nu^2)$ and so

$$a = -\frac{c_2^2 \pi}{c_4^2 L_2} \frac{1}{\nu} + \mathcal{O}(\nu), \quad b = \frac{L_1^4 c_2^2}{\pi^2 (4L_1^2 + L_2^2)} \frac{1}{\nu} + \mathcal{O}(\nu)$$

hence the radius of the stable limit cycle for small $-\mu_1$ is

$$\frac{\pi}{L_1^2 c_4} \left(\frac{4L_1^2 + L_2^2}{L_2} \right)^{\frac{1}{2}} (-\mu_1)^{\frac{1}{2}} + \mathcal{O}(\nu^{\frac{1}{2}}).$$

This concludes the proof. \square

We finally provide the proof of Theorem 4.3.

Proof. [Theorem 4.3] In order to unfold in μ_2 , we cannot cite a center manifold theorem from [12] verbatim. The reason is that μ_2 modifies the second order derivative terms, but the results in [12] are formulated for parameter dependence of lower order terms only. However, as pointed out in [12, Remark 3.7], there is no problem if the domain of \mathbf{L} is independent of the parameter. This is the case here as long as $\nu = \nu_{\text{crit}}(1) - \mu_2^2 > 0$, which is valid for the purpose of unfolding from $\nu = \nu_{\text{crit}}$. More precisely, the proof of [12, Theorem 3.3, p. 46], which considers the phase space extended by the unfolding parameter space, applies as follows for $\nu_{\text{crit}}(1) > \mu_2^2$ due to the linearity in μ_2^2 . Set $\mu = (\mu_1, \mu_2^2)$, $\tilde{u} = (u, \mu)$ and $\tilde{\mathbf{L}}\tilde{u} = (\mathbf{L} + \mu_1 \partial_{x_2}(u_1, 0)^T - \mu_2^2 \nabla^2 u, 0)$ as well as $\tilde{R}(\tilde{u}) = (R(u), 0)$, where $\Delta\nu = 0$. (We use μ_2^2 as the parameter instead of μ_2 only to get more pleasant reduced equations.) For the extended problem, the parameter-free center manifold theorem applies [12, Theorem 2.9].

Therefore, as in the first part of the proof of Theorem 3.4, we obtain existence of the center manifold and the coefficient b is unchanged. Let A denote the real coefficient of z in the vector field on the center manifold. It remains to derive the claimed a_j -dependent form

$$A = a_1 \mu_1 (a_2 \mu_2 - a_3 \mu_1) + \mathcal{O}(\mu_2^2 + |\mu_1 \mu_2^3|).$$

For this we simply note that in the present case, (4.10) is replaced by the more general form

$$A = \langle R_{11}(\zeta)\mu, \zeta^* \rangle_2 = \mu_1 a - \mu_2^2 \langle \nabla^2 \zeta, \zeta^* \rangle_2,$$

where $\zeta = \xi g_{1,1}$. Using $\nabla^2 g_{1,1} = -\pi^2 \left(\frac{1}{L_1^2} + \frac{4}{L_2^2} \right) g_{1,1}$ as well as $\langle \zeta, \zeta^* \rangle_2 = 1$, we obtain

$$A = \mu_1 a + \mu_2^2 \pi^2 \left(\frac{1}{L_1^2} + \frac{4}{L_2^2} \right) = \mu_1 a + \mathcal{O}(\mu_2^2), \quad (4.23)$$

with a from Theorem 4.1, whose dependence on μ_2 is considered next. Recall that $\nu = \nu_{\text{crit}} - \mu_2^2$, with $\mu_2 = 0$ giving equality in (3.13). Hence,

$$\nu_{\text{crit}} = \frac{2}{\pi L_1 L_2 \tilde{c}_3^2},$$

where \tilde{c}_3 stems from writing

$$d(\Delta T, 1)/L_1^4 = (2\tilde{c}_1 - \tilde{c}_2 \Delta T) \Delta T - \nu^2 \tilde{c}_3^2,$$

with suitably defined \tilde{c}_j , $j = 1, 2, 3$ (note the relation to c_j in (4.1)). Then $d(\Delta T, 1) = 0$ gives

$$\Delta T_{\text{crit}} = \tilde{c}_1 + \frac{\tilde{c}_3}{2} \mu_2 \sqrt{2\nu_{\text{crit}} - \mu_2^2}.$$

Using (4.22) with $\Delta T = \Delta T_{\text{crit}} + \mu_1$ then yields

$$a = a_1 \left(\tilde{c}_3 \mu_2 \sqrt{2\nu_{\text{crit}} - \mu_2^2} - 2\tilde{c}_2 \mu_1 \right).$$

The above formula for ν_{crit} and expansion in $\mu_2 = 0$ gives claimed form of A , when substituting the resulting a into (4.23). Employing the symmetry as in the proof of Theorem 3.4 implies the form of reduced equations.

The bifurcation scenario can be immediately read off the reduced vector field as follows: Let us fix μ_2 with $0 < |\mu_2| \ll 1$ and set $\Delta\nu = 0$. Then the reduced vector field shows that at the stability thresholds we have supercritical bifurcations. In the instability region of the equilibrium $r = 0$ the stable limit cycle radii are

$$r = \sqrt{\frac{a_1\mu_1(a_3\mu_1 - a_2\mu_2)}{b}},$$

which gives the connected branch of periodic orbits with endpoints at the bifurcations, perturbed for $0 < \Delta\nu \ll |\mu_2|$. \square

5. Travelling waves and Turing instabilities. As mentioned before, due to the translation symmetry in x_2 , the Andronov-Hopf bifurcations correspond to periodic travelling wave bifurcations and each periodic orbit is a steady state in a comoving frame $y_2 = x_2 - st$ for certain s . While this relation is generally known for completeness we give some details. The converse is clear: non-stationary periodic travelling wave bifurcations imply Andronov-Hopf-type bifurcations.

First note that the effect of the co-moving variable is the introduction of an advection term $s\partial_{y_2}$ on the right hand side of the first two equations in (1.1). Therefore, the linearization M_k is replaced by

$$M_{k,s} = M_k + sC_1(k)\text{Id},$$

where $C_1(k) = 2\pi ik_2/L_2$. Hence, if λ_k is an eigenvalue of M_k then $\lambda_k + sC_1(k)$ is an eigenvalue of $M_{k,s}$ and choosing critical $k_2 = +1$, the frequency at bifurcation ω is replaced by $\omega + s2\pi/L_2$. The reduced equation on the center manifold then reads

$$\dot{z} = i(\omega + s2\pi/L_2)z + \mu_1 a + bz|z|^2,$$

where a and b are unmodified since the matrices made of c_j in (4.15) *do not* depend on s . Hence, for $s = s_* := -\omega L_2/2\pi$ we find steady state supercritical pitchfork bifurcations in the amplitude. Note the choice $k_2 = -1$ reverses the sign of ω , simply leading to the complex conjugate equation.

Since the spectrum of the modified \mathbf{L} possesses a *double zero* eigenvalue at $s = s_*$, the coefficients on the center manifold are not immediately given by the Andronov-Hopf case used above. However, the reduced vector field on the 2D center manifold of the double zero eigenvalue reduces further to a scalar equation, undergoing a pitchfork bifurcation, precisely due to the translation symmetry: In polar coordinates of the Hopf normal form, this is due to detuning the trivial angular equation, co-rotation with velocity $sC_1(1)$, to stationarity. The co-moving frame speed in the unfolding generically depends on the amplitude. An exception are $O(2)$ -symmetric cases such as $\Delta\nu = 0$ as discussed previously.

In the context of travelling waves, let us briefly take the perspective of pattern formation, for which the infinite strip $x \in [0, L_1] \times \mathbb{R}$ is the natural domain here. The linear stability analysis of the laminar steady state in this case involves the eigenvalues λ_k^\pm from §3 with $k = (k_1, k_2)$ where k_2 is continuous and rescaled: these are now eigenmodes in the essential spectrum given by λ_k^\pm with $k = (k_1, L_2 k_2)$, $(k_1, k_2) \in \mathbb{N}_* \times \mathbb{R}$.

We are then lead to search for pattern-forming instabilities, and indeed, the system allows for the analogue of Turing instabilities from reaction-diffusion systems, which is also well known in fluid dynamics, for instance Rayleigh-Bénard convection. For $\Delta\nu = 0$, as for the finite dimensional bifurcation discussed in the previous sections, the symmetry enters and turns Turing-Hopf instabilities fully into Turing instabilities in a suitable frame of reference. The spectral configuration of a Turing-Hopf instabilities in general is such that the essential spectrum touches the imaginary axis at some $\lambda = \lambda(k_1, k_2)$ with $\Im(\lambda) \neq 0$, $(k_1, k_2) \neq 0$, and crosses it upon parameter variation; for a Turing instability the critical spectrum is real. Due to Lemma 3.1 critical eigenmodes must have $k_1 = 1$. More precisely, we have the following, where supercritical refers to positive real part of the Landau-coefficient in the associated Grinzburg-Landau amplitude equations. For the general theory of these equations for pattern forming instabilities we refer to [5, 23].

LEMMA 5.1. *For $0 \leq \Delta\nu \ll 1$ and any fixed $L_1 > 0$ there exists a unique $\nu_{\text{TH}} > 0$ such that the laminar steady state is stable for $\nu > \nu_{\text{TH}}$ and all ΔT . For $0 < \nu < \nu_{\text{TH}}$ it undergoes supercritical Turing-Hopf instabilities at precisely two values of ΔT , and these lie in $(0, \Delta T_*)$. For $\Delta\nu = 0$ and in the reference frame of Remark 1 these are pure Turing instabilities. The critical eigenmodes have wavenumber $k_1 = 1$ and some $k_2 = k_2(\Delta T)$, and the imaginary part of the critical eigenmode (the frequency) is $\Delta T \pi k_2(\Delta T)$.*

For fixed L_1 and any $\Delta T \in (0, \Delta T_)$, a Turing-Hopf instability occurs at a unique ν , and there is no instability in ν for $\Delta T < 0$ or $\Delta T \geq \Delta T_*$.*

Proof. As before we may and will set $\nu = 0$ due to smoothness. Recall that for bounded rectangular domains, the function $d(\Delta T, k_2^2)$ from (3.12) has the sign of $\Re(\lambda_{(1, k_2)}^+)$. This followed from (3.10), which in the case of an infinite strip has k_2 replaced by $k_2 L_2$, where k_2 is now the continuous wavenumber. Then ℓ is replaced by $1/L_1$ in (3.10) so that $d(\Delta T, k_2^2)$ gives the sign of critical modes for the infinite strip when setting $\ell = 1/L_1$. The scaling also implies that given an instability, the claimed critical frequency follows from (3.1) with k_2 replaced by $L_2 k_2$.

Lemma 3.2 shows that instabilities can occur for $\Delta T \in [0, \Delta T_*)$ only, and $\Delta T = 0$ requires $\nu = 0$. Due to Lemma 3.7, for any $\nu \geq 0$, the graph of $d : \mathbb{R} \times \mathbb{R}^+ \rightarrow \mathbb{R}$ is parabolic. In particular, there is a unique maximum of $d(\Delta T, k_2^2)$, and it has $k_2 > 0$. Hence, the maximal real part of the spectrum lies at a unique $(\Delta T, k_2)$, and for the lemma it now suffices (by continuity) to find values of ν where the maximum of $d(\Delta T, k_2^2)$ is positive and where it is negative.

For $\nu = 0$ the maximum is positive since then (3.13) holds, and it is bounded as a function of k_2^2 (with maximum at $k_2 = 0$). For $\nu > 0$ the additional term in $d(\Delta T, k_2^2)$ is the negative contribution

$$-\nu^2 \pi^4 \frac{(4\kappa_2 + \ell^2)^2}{\kappa_2 \ell^4}$$

which is bounded from above as a function of κ_2 (with maximum at $\kappa_2 = \ell^2/4$). Hence, ν can be chosen so large, that $d(\Delta T, \kappa_2) < 0$ for all $\Delta T, \kappa_2 \geq 0$.

Since the periodic solutions of §4 always bifurcate supercritically implies that the Turing(-Hopf) instabilities are supercritical: with $L_2 = 2\pi/k_{\text{TH}}$ the mode with critical wavenumber is the lowest spatial harmonic and the supercritical Andronov-Hopf bifurcation implies positive real part of the Landau-coefficient in the Grinzburg-Landau amplitude equations. \square

A numerically computed example is given in Figure 5.1, which is derived from

that in Figure 3.2(a). Here the critical modes at onset of the instability on the infinite strip have wavenumber near 0.75.

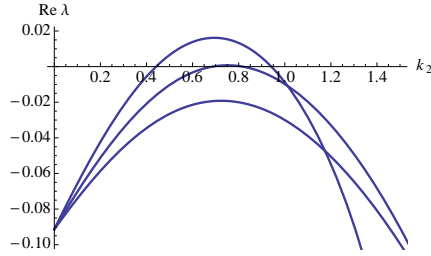


FIG. 5.1. A Turing(-Hopf) instability for parameters as in Figure 3.2(a): real parts of eigenvalues λ_k^+ , $k = (1, k_2)$, as functions of k_2 for $\Delta T = 0.05$ (stable), $\Delta T = 0.08$ (near bifurcation) and $\Delta T = 0.2$ (unstable).

6. Nonlinear Instability. In this short paragraph, we give some details on the fact that the linear instability of the laminar state ρ_{ss} is indeed an instability for the nonlinear equation uniformly in ν . Roughly speaking, this means that in $(\Delta T_1, \Delta T_2)$, there are initial data which are arbitrarily close to the steady state and which get “far” from it exponentially quickly. We thus assume $\Delta T_1 < \Delta T_2$ and take $\Delta T \in (\Delta T_1, \Delta T_2)$. This means that $\sigma_+(\mathbf{L}) \neq \emptyset$ (see the proof of Theorem 3.4).

In the parabolic formulation (2.5), the sectoriality of \mathbf{L} allows to apply the well known nonlinear instability results from [14] for spectrum in the right half plane. However, this heavily relies on $\nu > 0$ and the following does not. Furthermore, the result given for the specific case here is actually stronger than the general ones in [14].

As in [10, Theorem 6.1], the following instability result holds for $\nu^\pm \geq 0$:

THEOREM 6.1. *Suppose $\Delta T \in (\Delta T_1, \Delta T_2)$. There exist constants $\delta_0, \eta_1, \eta_2 > 0$ such that for any $0 < \delta < \delta_0$ and any $s \geq 0$ there exists a solution (ρ^\pm, E) to (1.1) with $\|\rho^\pm(0) - \rho_{ss}^\pm\|_{H^s} \leq \delta$ but such that:*

$$\|\rho^\pm(t_\delta) - \rho_{ss}^\pm\|_{L^2} \geq \eta_1 \text{ and } \|E(t_\delta)\|_{L^2} \geq \eta_2,$$

with $t_\delta = O(|\log \delta|)$.

In order to pass from linear to nonlinear instability, a natural candidate is the solution (ρ^\pm, E) to (1.1) with initial datum

$$\rho^\pm(0) = \rho_{ss}^\pm + \delta h^\pm,$$

where (h^+, h^-) is an eigenfunction associated to an eigenvalue λ_1 with maximal real part for the linearized operator. We expect the solution ρ^\pm to behave like the solution of the linearized equations:

$$\rho_{lin}^\pm(t) = \rho_{ss}^\pm + \delta e^{\lambda_1 t} h^\pm.$$

Since the nonlinear part of (1.1) involves derivatives, controlling the error between ρ^\pm and the approximation ρ_{lin}^\pm is not straightforward; the main idea is to apply the method of Grenier [8], whose principle is to build a more precise approximation of ρ^\pm , which allows to get a better control on the nonlinearities. Since the proof is identical to that of Theorem 6.1 in [10], we refer to this paper for details.

7. Global Nonlinear Stability. Let us now investigate the stability of the steady state ρ_{ss} , outside of $[\Delta T_1, \Delta T_2]$. We first state the results and then give the proofs.

The key point is the following energy identity for $M := \max(\nu_+, \nu_-)$ and $m := \min(\nu_+, \nu_-)$:

LEMMA 7.1. *For any initial data $\rho_0 \in L^\infty$, we have the following estimate for the energy of the system (1.1)*

$$\begin{aligned} \mathcal{E}(t) &:= \|\rho - \rho_{ss}\|_{L^2}^2 - \frac{2}{L_1 \Delta T} \int_{\Omega} |\nabla V|^2 dx \\ &+ 2 \int_0^t \left[\frac{-4M}{L_1 \Delta T} \|\rho - \rho_{ss}\|_{L^2}^2 + m \|\nabla(\rho - \rho_{ss})\|_{L^2}^2 \right] ds \\ &\leq \mathcal{E}(0) = \|\rho_0 - \rho_{ss}\|_{L^2}^2 - \frac{2}{L_1 \Delta T} \int_{\Omega} |\nabla V|_{t=0}|^2 dx, \end{aligned} \quad (7.1)$$

with $\|\rho - \rho_{ss}\|_{L^2}^2 = \|\rho^+ - \rho_{ss}^+\|_{L^2}^2 + \|\rho^- - \rho_{ss}^-\|_{L^2}^2$, $\|\nabla(\rho - \rho_{ss})\|_{L^2}^2 = \|\nabla(\rho^+ - \rho_{ss}^+)\|_{L^2}^2 + \|\nabla(\rho^- - \rho_{ss}^-)\|_{L^2}^2$ and $\nabla V = -\nabla(\nabla^2)^{-1}(\rho^+ + \rho^- - 1)$.

REMARK 11. *We take the opportunity to point out an error in the energy of [10, Theorem 5.1]: in equations (5.1) and (5.2) of this paper, there is a factor 2 which is missing in front of $\int_{\Omega} |\nabla V|^2 dx$.*

We shall use in the following Poincaré type inequalities:

LEMMA 7.2. *With the same notations as before, we have, for any $t \geq 0$:*

$$\|\nabla V\|_{L^2}^2 \leq \frac{2L_1^2}{\pi^2} \|\rho - \rho_{ss}\|_{L^2}^2, \quad (7.2)$$

$$\|\rho - \rho_{ss}\|_{L^2}^2 \leq \frac{L_1^2}{\pi^2} \|\nabla(\rho - \rho_{ss})\|_{L^2}^2. \quad (7.3)$$

As a consequence of the energy identity, we can prove L^2 -return to equilibrium, with exponential (and explicit) speed, for negative or large enough ΔT .

THEOREM 7.3. *If $\Delta T < 0$ or $\Delta T > \Delta T_* := \frac{4L_1}{\pi^2} \max\left(\frac{\nu_+}{\nu_-}, \frac{\nu_-}{\nu_+}\right)$, then the steady state ρ_{ss} is globally asymptotically stable in L^2 , with exponential convergence rate*

$$-2 \min(\nu_+, \nu_-) \frac{\pi^2}{L_1^2} - \frac{4\pi^2 |\nu_+ - \nu_-|}{L_1(\pi^2 \Delta T - 4L_1)}.$$

REMARK 12. *Notably, the constants in all these results are independent of L_2 , and the convergence rate is larger on thinner domains (with smaller L_1), but also balancing with viscosity.*

Recall that by Lemma 3.2, for fixed $\ell = L_2/L_1$ the upper instability threshold ΔT_2 satisfies $\Delta T_2 < \Delta T_* = \frac{4L_1}{\pi^2}$, but that $\lim_{\ell \rightarrow +\infty} \Delta T_2 = \Delta T_*$ if $\nu = o(\ell^{-1})$. Hence, the global threshold estimate ΔT_* is also linked to linear instability.

Let us now prove Lemma 7.1, Lemma 7.2 and Theorem 7.3.

Proof. [Lemma 7.1] The proof follows from computations that are similar to those that can be found in [10], for the model without viscosity (that is $\nu_+ = \nu_- = 0$). We keep the notations of Section 2.

Taking the scalar product with $u := (u_1, u_2)$ in the transport equations satisfied by u_1 and u_2 in (2.1), and integrating with respect to x entails

$$\frac{1}{2} \frac{d}{dt} \|u\|_{L^2}^2 = \int_{\Omega} \frac{E_2}{L_1} u_1 dx - \int_{\Omega} \frac{E_2}{L_1} u_2 dx + \nu_- \int_{\Omega} u_1 \nabla^2 u_1 dx + \nu_+ \int_{\Omega} u_2 \nabla^2 u_2 dx. \quad (7.4)$$

Note indeed that due the periodicity with respect to x_2 , the following contribution vanishes:

$$\int_{\Omega} \partial_{x_2} u_1 u_1 dx = \int_{\Omega} \frac{1}{2} \partial_{x_2} u_1^2 dx = 0 = \int_{\Omega} \partial_{x_2} u_2 u_2 dx.$$

Likewise, with Green's Formula, using $\operatorname{div} E^\perp = 0$ and $E_2 = -\partial_{x_2} V = 0$ on $x_1 = 0, L_1$, we have (for $i = 1, 2$)

$$\int_{\Omega} E^\perp \cdot \nabla u_i u_i dx = \frac{1}{2} \int_{\Omega} E^\perp \cdot \nabla (u_i)^2 dx = 0.$$

Recall an identity proved in [10, Lemma 5.1] for any $t > 0$, there holds

$$\int_{\Omega} E_2 u_1 dx = - \int_{\Omega} E_2 u_2 dx. \quad (7.5)$$

For the sake of completeness, we quickly reproduce the proof. Observe that

$$\begin{aligned} \int_{\Omega} E_2 (u_2 - u_1) dx &= \int_{\Omega} E_2 (u_1 + u_2 - 2u_1) dx \\ &= \int_{\Omega} E_2 (-\nabla^2 V - 2u_1) dx = -2 \int_{\Omega} E_2 u_1 dx. \end{aligned} \quad (7.6)$$

Indeed, due to periodicity in the x_2 -direction and since $\partial_{x_2} V = 0$ on $x_1 = 0, L_1$, we get

$$\begin{aligned} \int_{\Omega} \partial_{x_2} V \nabla^2 V dx &= - \int_{\Omega} \partial_{x_2} \nabla V \cdot \nabla V dx + \underbrace{\int_{\Omega} \operatorname{div}(\partial_{x_2} V \nabla V) dx}_{=0} \\ &= - \int_{\Omega} \partial_{x_2} \left(\frac{|\nabla V|^2}{2} \right) dx = 0. \end{aligned}$$

This completes the proof of (7.5) and therefore, we have

$$\int_{\Omega} -\frac{E_2}{L_1} u_1 dx + \int_{\Omega} \frac{E_2}{L_1} u_2 dx = -2 \int_{\Omega} \frac{E_2}{L_1} u_1 dx.$$

Now compute, using the equations satisfied by (u_1, u_2, V) :

$$\begin{aligned} \int_{\Omega} E_2 u_1 dx &= \int_{\Omega} V \partial_{x_2} u_1 dx - \underbrace{\int_{\Omega} \operatorname{div}(V u_1 e_2) dx}_{=0} \\ &= \frac{1}{\Delta T} \int_{\Omega} V \left(\partial_t u_1 + E^\perp \cdot \nabla u_1 - \frac{E_2}{L_1} \right) dx - \frac{\nu_-}{\Delta T} \int_{\Omega} V \nabla^2 u_1 dx \\ &= \frac{1}{\Delta T} \int_{\Omega} V (\partial_t (u_1 + u_2) + E^\perp \cdot \nabla (u_1 + u_2)) dx \\ &\quad - \frac{1}{\Delta T} \int_{\Omega} V \nabla^2 (\nu_- u_1 + \nu_+ u_2) dx \\ &= \frac{1}{\Delta T} \int_{\Omega} -V (\partial_t \nabla^2 V - E^\perp \cdot \nabla (\nabla^2 V)) dx \\ &\quad - \frac{1}{\Delta T} \int_{\Omega} V \nabla^2 (\nu_- u_1 + \nu_+ u_2) dx. \end{aligned} \quad (7.7)$$

Observe that by Green's formula

$$\int_{\Omega} -V (\partial_t \nabla^2 V - E^\perp \cdot \nabla(\nabla^2 V)) dx = \frac{d}{dt} \frac{1}{2} \left(\int_{\Omega} |\nabla V|^2 dx \right)$$

and using again (7.5), we have

$$\int_{\Omega} \frac{E_2}{L_1} (u_1 - u_2) dx = \frac{1}{L_1 \Delta T} \frac{d}{dt} \left(\int_{\Omega} |\nabla V|^2 dx \right) dx - \frac{2}{L_1 \Delta T} \int_{\Omega} V \nabla^2 (\nu_- u_1 + \nu_+ u_2) dx.$$

Note that using Green's formula and the Poisson equation satisfied by V , we have

$$\int_{\Omega} V \nabla^2 (\nu_- u_1 + \nu_+ u_2) dx = \int_{\Omega} \nabla^2 V (\nu_- u_1 + \nu_+ u_2) dx \geq -2M \|u\|_{L^2}^2$$

since $(u_1 + u_2)(\nu_- u_1 + \nu_+ u_2) \leq 2 \max(\nu_-, \nu_+) (u_1^2 + u_2^2)$.

Finally, gathering all pieces and using

$$\int_{\Omega} u_j \nabla^2 u_j dx = - \int_{\Omega} |\nabla u_j|^2 dx$$

we have proven that $\frac{d}{dt} \mathcal{E}(t) \leq 0$. \square

Let us now prove the Poincaré inequalities of Lemma 7.2.

Proof. [Lemma 7.2] We prove (7.2) only since (7.3) can be treated similarly. Using the orthogonal basis (3.3), we write:

$$u_1 + u_2 = \sum_{k_1 \in \mathbb{N}_*, k_2 \in \mathbb{Z}} a_{k_1, k_2} g_k.$$

Recall the Poisson equation satisfied by V : $-\nabla^2 V = u_1 + u_2$. This yields:

$$V = \sum_{k_1 \in \mathbb{N}_*, k_2 \in \mathbb{Z}} \frac{1}{\pi^2 \left(\frac{k_1^2}{L_1^2} + \frac{4k_2^2}{L_2^2} \right)} a_{k_1, k_2} g_k,$$

$$\nabla V = \sum_{k_1 \in \mathbb{N}_*, k_2 \in \mathbb{Z}} \frac{1}{\pi^2 \left(\frac{k_1^2}{L_1^2} + \frac{4k_2^2}{L_2^2} \right)} a_{k_1, k_2} \pi \left(\frac{k_1}{L_1} \phi_k \right).$$

Therefore,

$$\int_{\Omega} |\nabla V|^2 dx \leq \frac{L_1^2}{\pi^2} \|u_1 + u_2\|_{L^2}^2 \leq \frac{2L_1^2}{\pi^2} (\|u_1\|_{L^2}^2 + \|u_2\|_{L^2}^2), \quad (7.8)$$

which proves (7.2). \square

Gathering all pieces together, we can now prove Theorem 7.3.

Proof. [Theorem 7.3] Using the energy identity (7.1) and applying the Poincaré inequality (7.2) we get:

$$\begin{aligned} \|u\|_{L^2}^2 &\leq \|u(0)\|_{L^2}^2 + \frac{2}{L_1 \Delta T} \int_{\Omega} |\nabla V|^2 dx - 2 \int_0^t \left[\frac{-4M}{L_1 \Delta T} \|u\|_{L^2}^2 + m \|\nabla u\|_{L^2}^2 \right] ds \\ &\leq \|u(0)\|_{L^2}^2 + \frac{1}{L_1 \Delta T} \frac{4L_1^2}{\pi^2} \|u\|_{L^2}^2 - 2 \int_0^t \left[\frac{-4M}{L_1 \Delta T} \|u\|_{L^2}^2 + m \|\nabla u\|_{L^2}^2 \right] ds. \end{aligned}$$

Hence, using the Poincaré inequality (7.3),

$$\left(1 - \frac{4L_1}{\pi^2 \Delta T}\right) \|u\|_{\mathbb{L}^2}^2 \leq \|u(0)\|_{\mathbb{L}^2}^2 + 2\nu \left(\frac{4M}{L_1 \Delta T} - m \frac{\pi^2}{L_1^2}\right) \int_0^t \|u\|_{\mathbb{L}^2}^2 ds.$$

As a consequence, by Gronwall inequality, we obtain \mathbb{L}^2 -stability and \mathbb{L}^2 -return to equilibrium, provided that

$$\Delta T < 0, \text{ or } \Delta T > \frac{4L_1 M}{\pi^2 m},$$

which in particular implies $m \frac{\pi^2}{L_1^2} - M \frac{4}{L_1 \Delta T} > 0$ and $\Delta T > \frac{4L_1}{\pi^2}$. More specifically:

$$\|u\|_{\mathbb{L}^2}^2 \leq \frac{4\pi^2}{L_1(\pi^2 \Delta T - 4L_1)} \|u(0)\|_{\mathbb{L}^2}^2 \exp(-\gamma t), \quad (7.9)$$

with $0 < \gamma := 2 \left(m \frac{\pi^2}{L_1^2} - \frac{4M}{L_1 \Delta T}\right) \left(1 - \frac{4L_1}{\pi^2 \Delta T}\right)^{-1} = 2m \frac{\pi^2}{L_1^2} - \frac{4\pi^2 |\Delta \nu|}{L_1(\pi^2 \Delta T - 4L_1)}$. \square

8. Numerical results. For illustration of the analytical results given in the previous sections we next discuss some numerical computations. In the first subsection we present numerical time integration using harmonic discretization and slow parameter ramping in order to approximate and track attractors. In the second subsection we show results of a complementary approach by numerical continuation, which allows to track stable and unstable branches more accurately, and also detect bifurcation points. In doing this, we mainly focus on the parameter set

$$\nu = 9 \cdot 10^{-4}, \quad L_1 = L_2 = 2, \quad \Delta \nu = 0, \quad (8.1)$$

which has $L_2 < 2\sqrt{2}L_1$ so that a primary 1-instability region $(\Delta T_1, \Delta T_2)$ exists (Theorem 3.4), and the endpoints of this are supercritical Hopf-bifurcations to traveling waves (Corollary 4.2). For parameters (8.1) we readily compute that $\Delta T_1 \approx 3 \cdot 10^{-4}$, $\Delta T_2 \approx 0.162$.

8.1. Time integration and parameter ramping. Here we discretized (2.1) with a finite-dimensional spectral decomposition

$$u_l(x, t) = \sum_{k_1=1}^{N_{x_1}} \sum_{k_2=-N_{x_2}}^{N_{x_2}} C_{k_1, k_2, l}(t) g_{k_1, k_2}(x), \quad l = 1, 2, \quad (8.2)$$

with harmonics g_k as defined in (3.3). We integrated the resulting system of ODEs for $C_{k_1, k_2, l}$ using a semi-implicit Crank-Nicolson scheme, where the linear part only is implicit¹. All the simulations were made with parameter values (8.1) and $N_{x_1} = N_{x_2} = 32$, and we selectively checked with $N_{x_1} = N_{x_2} = 64$.

¹We modified a code by Jean-Christophe Nave - MIT Department of Mathematics, jcnave@mit.edu for Navier-Stokes equations in vorticity formulation.

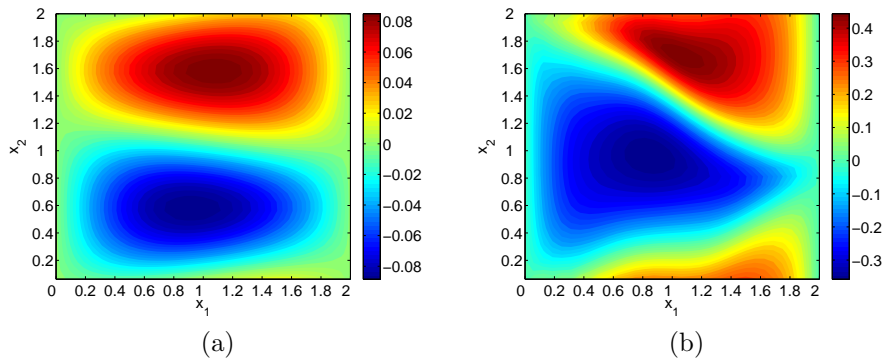


FIG. 8.1. Contour plots of $u_1(t_2) = \rho_1(t_2) - \rho_{ss}$ with $t_2 \approx 1000$, $\Delta T \in (\Delta T_1, \Delta T_2)$ and parameters as in (8.1). (a) the dynamics is a translation in the periodic x_2 -direction, $\Delta T = 0.159291$ is close to the upper instability threshold, and (b) $\Delta T = 0.146122$, the dynamics resembles a modulated travelling wave, moving in the x_2 direction.

In Figure 8.1 we plot one solution near the upper stability threshold $\Delta T_2 \approx 0.162$ and another further inside the nonlinear regime as can be seen by the locus of parameters in Figure 8.2(a). The ‘weakly nonlinear’ solution for $\Delta T \approx \Delta T_2$ closely resembles the unstable eigenfunction and appears to be a periodic travelling wave as predicted by the theory. The solution further inside the nonlinear regime has a clear nonlinear structure and does not appear to be close to a travelling wave: it has additional oscillations superimposed to the drift. Indeed, the numerical results of §8.2 indicate that the travelling waves in this parameter region are unstable.

Here we located and tracked the solutions emerging from the supercritical bifurcation at $\Delta T = \Delta T_1$, by a simple parameter ramping: for ΔT near the bifurcation at ΔT_1 , we simulate an initial condition close to ρ_{ss} and after a transient, $t = t_1 \approx 400$, we compute the maximum over the interval $[t_1, 1000]$. Next, we slightly increase ΔT and repeat this step with the initial condition being the solution at the final time of the previous step. In this way we obtain the ‘ramping diagram’ in Figure 8.2(a), for which we used 100 ramping steps with smaller stepsize near the endpoints. As predicted by Theorem 4.1, the slope of the ramping curve is larger near the left endpoint of the instability region than near the right endpoint. The numerical instability thresholds of the laminar state are in good agreement with the analytical ones with better accuracy near the right endpoint. Further away from these thresholds, solutions are no longer travelling waves as noted above and corroborated by the time trace of the domain mid-point plotted in Figure 8.2(b). However, when continuing the ramping the solution still turns into the near harmonic periodic solution bifurcating from the right endpoint ΔT_2 . Compare Figure 8.1 (a).

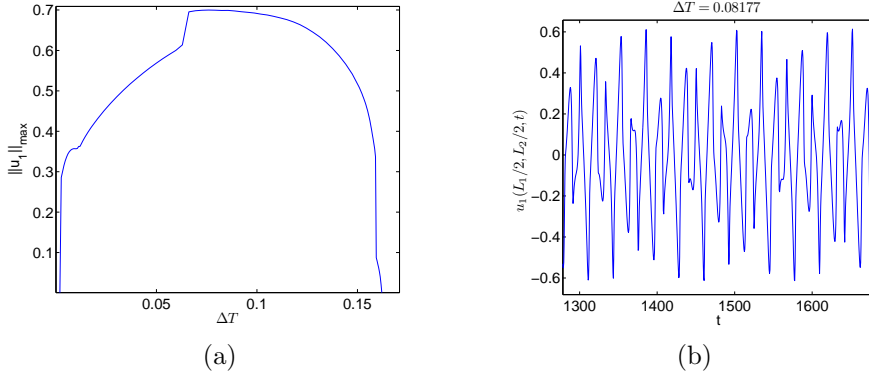


FIG. 8.2. (a) Ramping diagram in ΔT with $\max_{t_1 \leq t \leq t_2} \|u_1(t)\|_\infty$ on the vertical axis, where $t_2 \approx 1000$. The parameters are as in (8.1), the diagram is in agreement with corollary 4.2. (b) Time trace of u_1 at the midpoint $(x_1, x_2) = (L_1/2, L_2/2)$ for $\Delta T = 0.08$

8.2. Numerical continuation. In this section we present a different approach to numerically illustrate and go beyond our analytical results. Instead of time integration we rely on numerical pseudo-arclength continuation which finds travelling waves by a Newton method. For some mathematical background on continuation, and the implementation in the finite elements based software package `pde2path` used here, we refer to [24] and to [6] for extensions that are relevant for our problem.

We thus study the stationary problem of (2.1) in a comoving frame $x_2 \mapsto x_2 - st$ with speed $s \in \mathbb{R}$, that is, the elliptic problem

$$\begin{cases} 0 = (\Delta T + s)\partial_{x_2}u_1 + E_2/L_1 - E^\perp \cdot \nabla u_1 + \nu \nabla^2 u_1, \\ 0 = s\partial_{x_2}u_2 - E_2/L_1 - E^\perp \cdot \nabla u_2 + (\nu + \Delta\nu)\nabla^2 u_2, \\ 0 = u_1 + u_2 + \nabla^2 V \end{cases} \quad (8.3)$$

with $E = (E_1, E_2) = -\nabla V$ and domain as well as boundary conditions of (2.1), and parameters (8.1).

We implemented this in `pde2path` (version 2) and used a regular 20×20 grid decomposed into right isosceles triangles and checked selected solutions with grids up to 100×100 . Using the analytical knowledge of the bifurcation points and critical eigenvector, we generated an initial guess for the continuation in ΔT . The resulting branches for $\nu = 9 \cdot 10^{-3}$ and $\nu = 9 \cdot 10^{-4}$ together with stability information are plotted in Figure 8.3(a,c); a solution contour is plotted in Figure 8.3(b).

As predicted by Theorem 4.1, the solutions are stable near the endpoints and the slope of the branch is larger near the left endpoint of the instability region than near the right endpoint. In case $\nu = 9 \cdot 10^{-3}$ the entire branch is stable, which is expected from Theorem 4.3, since ν is close to $\nu_{\text{crit}} \approx 0.01$, where the instability region vanishes.

Beyond the theory, the results for $\nu = 9 \cdot 10^{-4}$ in Figure 8.3(c) show that the travelling wave solutions destabilize away from the endpoints (apparently by symmetry breaking pitchfork bifurcations). In Figure 8.4 we plot the branches that bifurcate here. The rightmost of these extends beyond ΔT_2 , turns around and connects to a fully unstable branch of solutions emerging from the laminar state with wavevector $k = (2, 1)$, which also connects to the leftmost of the additional branches. We also mention that along the unstable branches there appear to be further destabilizations

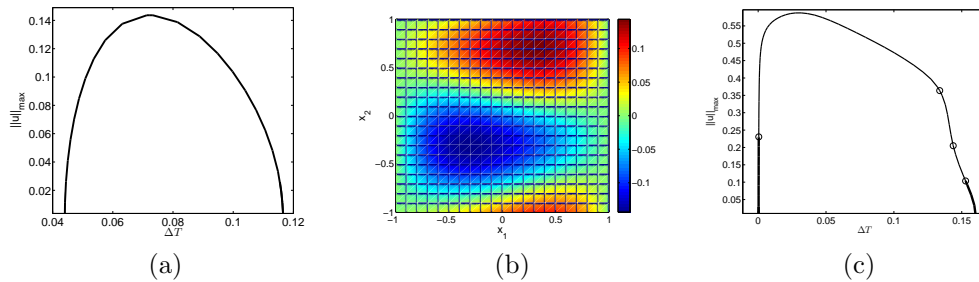


FIG. 8.3. (a) Branch of travelling waves for $L_1 = L_2 = 2$ for $\nu = 9 \cdot 10^{-3}$; all solutions are stable. (b) Contour plot of the u_1 -component of the travelling wave from (a) at $\Delta T = 0.07$. (c) Branch as in (a) but with $\nu = 9 \cdot 10^{-4}$; thick lines mark stable solutions, thin lines unstable ones and circles mark bifurcation points.

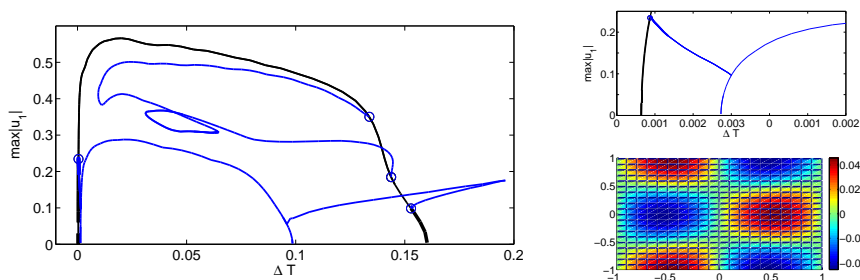


FIG. 8.4. Left panel: Bifurcation diagram as in Figure 8.3(c) with additional branches (blue) emerging from the bifurcation points of the primary branch; notably extending to $\Delta T > \Delta T_2$. Right upper panel: Magnification of left panel near $\Delta T = 0$. Right lower panel: u_1 -component of the small amplitude solution on the blue branch near $\Delta T = 0.1$ showing the wavevector $k = (2, 1)$.

by Hopf-bifurcations and thus much richer bifurcation diagrams than our present numerical computations can reveal.

In conclusion, the numerical results nicely corroborate the rigorous local analysis concerning stability, location and supercritical nature of bifurcations from the laminar state. Moreover, these results suggest that many other bounded solutions exist for small ν , in particular also for values of $\Delta T \in (\Delta T_2, \Delta T_*)$ between the upper linear and the estimated global stability thresholds. The latter would explain the necessity of a difference between the local and global stability thresholds of the laminar state.

REFERENCES

- [1] A.R. Adams, J.J.F. Fournier, *Sobolev spaces*, second ed., Pure and Applied Mathematics (Amsterdam), vol. 140, Elsevier/Academic Press, Amsterdam, 2003.
- [2] G.K. Batchelor, *An introduction to fluid dynamics*, Cambridge, 2000.
- [3] P. Braasch, G. Rein, J. Vukadinovic, *Nonlinear stability of stationary plasmas-an extension of the energy-Casimir method*, SIAM J. Appl. Math. **59** (1999) no. 3, 831–844.
- [4] K. H. Burrell. Effects of $E \times B$ velocity shear and magnetic shear on turbulence and transport in magnetic confinement devices. Phys. Plasmas **4** (1997) no. 5, 1499–1518.
- [5] M.C. Cross, P.C. Hohenberg, Pattern formation outside equilibrium, Rev. Mod. Phys. **65** (1993) 851–1112.
- [6] T. Dohnal, J.D.M. Rademacher, H. Uecker and D. Wetzel. *pde2path-V2: multi-parameter continuation and periodic domains*. In: H. Ecker, A. Steindl, S. Jakubek (eds.) ENOC 2014 - Proceedings of 8th European Nonlinear Dynamics Conference.

- [7] H. Goedbloed, S. Poedts, *Principles of Magnetohydrodynamics: With Applications to Laboratory and Astrophysical Plasmas*. Cambridge University Press, Cambridge, 2004.
- [8] E. Grenier, *On the nonlinear instability of Euler and Prandtl equations*, Comm. Pure Appl. Math. **53** (2000), no. 9, 1067–1091.
- [9] P. N. Guzdar, R. G. Kleva, and Liu Chen. *Shear flow generation by drift waves revisited*. Phys. Plasma **8** (2001)
- [10] D. Han-Kwan, *On the confinement of a tokamak plasma*, SIAM J. Math. Anal. **42** (2010), no. 6, 2337–2367.
- [11] D. Han-Kwan, *Quasineutral Limit of the Vlasov-Poisson System with Massless Electrons*, Communications in Partial Differential Equations, Volume 36, Issue 8, 2011, 1385-1425.
- [12] M. Haragus and G. Iooss, *Local bifurcations, center manifolds, and normal forms in infinite-dimensional dynamical systems*, Universitext, Springer-Verlag London Ltd., London, 2011.
- [13] A. Hasegawa and M. Wakatani, *Plasma edge turbulence*, Phys. Rev. Lett., 50 (1983) 682–686.
- [14] D. Henry, *Geometric theory of semilinear parabolic equations*, Lecture Notes in Mathematics, vol. 840, Springer-Verlag, Berlin, 1981.
- [15] P. Hirschberg and E. Knobloch, *Mode interaction in large aspect ratio convection*, Nonlinear Science no. 7, 1997, 537–556.
- [16] M.A. Malkov and P.H. Diamond, *Weak hysteresis in a simplified model of the L-H transition*, Phys. Plasmas 16, 012504, 2009.
- [17] A. Mouton, *Expansion of a singularly perturbed equation with a two-scale converging convection term*. arXiv preprint arXiv:1404.4262 (2014).
- [18] T. Nguyen, W. Strauss, *Linear stability analysis of a hot plasma in a solid torus*, Archive for Rational Mechanics and Analysis, 211(2), 2014, 620-671.
- [19] Y. Sarazin, V. Grandgirard, E. Fleurence, X. Garbet, Ph. Ghendrih, P. Bertrand and G. Depret, *Kinetic features of interchange turbulence*, Plasma Phys. Control. Fusion 47 1817, 2005.
- [20] Y. Sarazin, V. Grandgirard, G. Dif-Pradalier, E. Fleurence, X. Garbet, Ph. Ghendrih, P. Bertrand, N. Besse, N. Crouseilles, E. Sonnendrücker, G. Latu and E. Violard, *Impact of large scale flows on turbulent transport*, Plasma Phys. Control. Fusion 48 B179, 2006.
- [21] B. Saltzman, *Finite amplitude free convection as an initial value problem-I*, Journal of atmospheric sciences 19, (1962) 329–341.
- [22] F. Wagner, *A quarter-century of H-mode studies*, Plasma Phys. Control. Fusion 49 B1, 2007.
- [23] I.S. Aranson, L. Kramer, *The world of the complex Ginzburg-Landau equation*. Rev. Mod. Phys. **74** (2002) 99–143.
- [24] H. Uecker, D. Wetzal, and J.D.M. Rademacher. pde2path – a Matlab package for continuation and bifurcation in 2D elliptic systems. Num. Math.: Th. Meth. Appl. 7 (2014) 58-106. Software at www.staff.uni-oldenburg.de/hannes.uecker/pde2path/
- [25] I. U. Uzun-Kaymak, P. N. Guzdar, R. Clary, R. F. Ellis, A. B. Hassam, and C. Teodorescu. *Analysis and modeling of edge fluctuations and transport mechanism in the Maryland Centrifugal Experiment*. Physics of Plasmas 15 (2008) 112308